



1 Long-term trends in pH in Japanese coastal waters

2

3 Miho Ishizu¹, Yasumasa Miyazawa¹, Tomohiko Tsunoda², Tsuneo Ono³

4

5 ¹E-mail: mishizu@jamstec.go.jp

6 ¹E-mail: miyazawa@jamstec.go.jp

7 Japan Agency for Marine-Earth Science and Technology, Environmental Variability Prediction and

8 Application Research Group, Yokohama Institute for Earth Sciences, 3173-25 Showa-machi,

9 Kanagawa-ku, Yokohama 236-0001, Japan

10 Tel: +81-45-778-5875

11 Fax: +81-45-778-5497

12

13 ²E-mail: t-tsunoda@spf.or.jp

14 The Ocean Policy Research Institute of the Sasakawa Peace Foundation, 1-15-16, Toranomom Minato-

15 ku, Tokyo 105-8524, Japan

16

17 ³E-mail: tono@affrc.go.jp

18 Japan Fisheries Research Education Agency, 15F Queen's Tower B, 2-3-3 Minato Mirai, Nishi-ku,

19 Yokohama, Kanagawa 220-6115, Japan

20

21 Abstract

22 In recent decades, acidification of the open ocean has shown consistent increases. However,

23 analysis of long-term data in coastal waters shows that the pH is highly variable because of coastal



24 processes and anthropogenic carbon inputs. It is therefore important to understand how anthropogenic
25 carbon inputs and other natural or anthropogenic factors influence the temporal trends in pH in coastal
26 waters. Using water quality data collected at 1481 monitoring sites as part of the Water Pollution
27 Control Program, we determined the long-term trends in pH in Japanese coastal waters at ambient
28 temperature from 1978 to 2009. We found that pH decreased (i.e., acidification) at between 70% and
29 75% of the sites and increased (i.e., basification) at between 25% and 30% of the sites. The rate of
30 decrease varied seasonally and was, on average, -0.0014 yr^{-1} in summer and -0.0024 yr^{-1} in winter,
31 but with relatively large deviations from these average values. While the overall trends reflect
32 acidification, watershed processes might also have contributed to the large variations in pH in coastal
33 waters. The seasonal variation in the average pH trends reflects variability in warming trends, while
34 regional differences in pH trends are partly related to heterotrophic water processes induced by nutrient
35 loadings.

36

37 Keywords: Ocean acidification, Coastal acidification/basification, pH, Data analysis,

38 CO₂

39

40 1. Introduction

41 The effect of ocean acidification on several marine organisms, including calcifiers, is widely

42 acknowledged and is the topic of various marine research projects worldwide. Chemical variables



43 related to carbonate cycles are monitored in several ongoing ocean projects to determine whether the
44 rate of ocean acidification can be identified from changes in pH and other variables in the open ocean
45 (Gonzalez-Davila et al. 2007; Dore et al. 2009; Bates 2007; Bates et al. 2014; Midorikawa et al. 2010;
46 Olafsson et al. 2009; Wakita et al. 2017). Analysis of pH data measured *in situ* at the European Station
47 in the Canary Islands (ESTOC) in the North Atlantic from 1995 to 2003 and normalized to 25°C
48 showed that pH_{25} decreased at a rate of $0.0017 \pm 0.0005 \text{ yr}^{-1}$ (Gonzalez-Davila et al. 2007). Similarly,
49 analysis of the Hawaii Ocean Time-series (HOT) (Dore et al. 2009) and the Bermuda Atlantic Time
50 Series (BATS) (Bates 2007) showed that pH at ambient sea surface temperature ($\text{pH}_{\text{in situ}}$) decreased by
51 0.0019 ± 0.0002 and $0.0017 \pm 0.0001 \text{ yr}^{-1}$ from 1988 to 2007 and from 1983 to 2005, respectively.
52 Analysis of data collected along the hydrographic observation line at 137°E in the western North
53 Pacific by the Japanese Meteorological Agency (JMA) showed that pH_{25} decreased by 0.0013 ± 0.0005
54 yr^{-1} in summer and $0.0018 \pm 0.0002 \text{ yr}^{-1}$ in winter from 1983 to 2007 (Midorikawa et al. 2010). The
55 winter $\text{pH}_{\text{in situ}}$ in surface water in the Nordic Seas decreased at a rate of $0.0024 \pm 0.0002 \text{ yr}^{-1}$ from 1985
56 to 2008 (Olafsson et al. 2009). This rate was somewhat more rapid than the average annual rates
57 calculated for the other subtropical time-series stations in the Atlantic Ocean, BATS, and ESTOC, and
58 was attributed to the air–sea CO_2 flux and buffering capacity (higher Revelle factor) (Olafsson et al.
59 2009), which were higher and lower than those in subtropical regions, respectively. Wakita et al. (2017)
60 estimated that the annual and winter $\text{pH}_{\text{in situ}}$ at station K2 in the subarctic western North Pacific
61 decreased at rates of 0.0025 and 0.0008 yr^{-1} , respectively, from 1999 to 2015. The lower rate in winter



62 was explained by increases in dissolved inorganic carbon (DIC) and total alkalinity (Alk) that resulted
63 from climate-related variations in ocean currents.

64 These long-term time-series from various sites in the open ocean indicate consistent changes in
65 surface ocean carbon chemistry, which mainly reflect the uptake of anthropogenic CO₂, with
66 consequences for ocean acidity. Coastal waters, however, differ from the open ocean as they are
67 subjected to multiple influences, such as hydrological processes, land use in watersheds, nutrient inputs
68 (Duarte et al. 2013), changes in the structure of ecosystems caused by eutrophication (Borges and
69 Gypens 2010; Cai et al. 2011), marine pollution (Zeng et al. 2015), and variations in salinity (Sunda
70 and Cai 2012).

71 Duarte et al. (2013) hypothesized that anthropogenic pressures would cause the pH_{insitu} of coastal
72 waters to decrease (acidification) or increase (basification), depending on the balance between the
73 atmospheric CO₂ inputs and watershed exports of alkaline compounds, organic matter, and nutrients.
74 For example, in Chesapeake Bay, trends in pH_{insitu} have shown temporal variations over the last 60
75 years, presumably because of the combined influence of increases and decreases in pH_{insitu} in the
76 mesohaline and polyhaline regions of the mainstem of the bay, respectively (Waldbusser et al. 2011;
77 Duarte et al. 2013). The pH_{insitu} in Tampa Bay increased consistently until 1980 but then dropped
78 almost instantly, only to gradually increase again (Duarte et al. 2013). The increases in pH_{insitu} until
79 1980 coincided with rapid increases in the population of the Tampa Bay watershed. In this period,
80 nutrients were not stripped from wastewater (Greening and Janicki 2006). However, a nutrient



81 management plan was implemented in 1980, and wastewater nutrient-removal was initiated. The sharp
82 decrease in $\text{pH}_{\text{in situ}}$ throughout the bay at this time might have been related to the decrease in primary
83 production triggered by the reduction in nutrients. In the period after 1980, $\text{pH}_{\text{in situ}}$ might have
84 increased again because of the expansion of seagrasses, improvements in water quality, and enhanced
85 CO_2 uptake (Duarte et al. 2013).

86 These processes that occur only in coastal regions might cause increases or decreases in the rate of
87 acidification, meaning that the outcomes for coastal ecosystems in different regions will vary. At
88 present we have limited information about long-term changes in pH in coastal waters, mainly because
89 of the difficulty involved in collecting continuous long-term data from coastal waters around an entire
90 country at a spatial resolution that is sufficient to cover the high regional variability in coastal pH.

91 The Water Pollution Control Law (WPCL) was established in 1970 to deal with the serious
92 pollution of the Japanese aquatic environment in the 1950s and 1960s. Several environmental variables,
93 including $\text{pH}_{\text{in situ}}$, have been continuously measured in coastal waters since 1978, using consistent
94 methods enacted in the monitoring program, to help protect coastal water and groundwater from
95 pollution and retain the integrity of water environments. The errors in pH measurements collected in
96 this program were assessed as outlined in the JIS Z8802 (JIS; Japanese Industrial Standard) standard
97 protocol (2011) that corresponds to the ISO 10523 (ISO; International Organization for
98 Standardization) standard protocol. Compared with the specialized oceanographic protocols described
99 in the United States Department of Energy (DOE) Handbook (1994), it is not difficult to achieve the



100 JIS protocol. The JIS and DOE standard protocols allow measurement errors of less than ± 0.07 and
101 ± 0.003 , respectively, for the glass electrode method, and the DOE protocol demands a precision of
102 ± 0.001 for the spectrophotometric method. Measurements are generally made with the higher-quality
103 spectrophotometric method during major oceanographic studies (e.g. Midorikawa et al. 2010). The
104 coastal monitoring program in Japan comprises more than 2000 monitoring sites that cover most parts
105 of the coastline (Fig. 1), so the dataset provides the opportunity to estimate the overall trend in pH in
106 Japanese coastal areas and the regional variability in the trends from data with a known precision.

107 In the present study, we examined the $\text{pH}_{\text{in situ}}$ trends in surface coastal waters from data measured
108 as part of WPCL monitoring programs. We then examined the trends at specific locations. The
109 remainder of this manuscript is organized as follows. The data and methods are described in Section
110 2, and trends in $\text{pH}_{\text{in situ}}$ are presented in Section 3. The results are discussed in Section 4 and the
111 concluding remarks are provided in Section 5.

112

113 2. Materials and Methods

114 2.1 Water Pollution Control Law (WPCL) monitoring data

115 Data for several environmental variables, including $\text{pH}_{\text{in situ}}$, and the associated metadata, are
116 available on the website of the National Institute for Environmental Studies (www.nies.go.jp/igreen;
117 http://www.nies.go.jp/igreen/md_down.html). We downloaded data for pH from 1978 to 2009 for the
118 trend analysis. We also downloaded temperature (T) and total nitrogen (TN) data that were measured



119 at the same sites as the pH data for the same time period (data for T and TN were available from 1981
120 and 1995, respectively), to check the quality of the pH_{insitu} data (Section 2.2), and to discuss coastal
121 processes that influenced the pH_{insitu} (Section 4.2).

122 The data were collected by the Regional Development Bureau of the Ministry of Land,
123 Infrastructure, Transport and Tourism, and the Ministry of the Environment under the WPCL
124 monitoring program. Monitoring protocols (sampling frequencies, locations, and methods) are outlined
125 in the program guidelines (NIES 2018; MOE 2018) written in Japanese, and here we summarize that
126 protocols.

127 Monitoring operations are occupied at 1481 sites along the Japan coast shown in Figure 1a. In
128 each monitoring sites, basic surveys were held 4 to 40 times a year dependent to the site. Information
129 on the sampling frequency at the monitoring sites is presented in Table 1. At each basic survey, water
130 samples were collected at several depths (0.5 and 2.0 m below the surface for all sites, and 10 m where
131 bottom depth was more than this) four times a day to cover diurnal variation. At sites where large
132 variation is found in the daily pH data, additional one day water sampling at 2-hourly intervals (ca. 13
133 times a day) was made at least twice a year to check the adequacy of basic water sampling protocol.

134 Measurements of pH for each water sample were made following the Japanese Industrial
135 Standard protocol JIS Z 8802 (2011), which is equivalent to ISO10523
136 (<https://www.iso.org/standard/51994.html>). Namely, pH was measured by glass electrode calibrated
137 by NBS standard buffers. Permitted repeatability in each measurement was ± 0.07 . NIES gathered all



138 pH data measured at each site and calculated annual minimum and maximum pH.

139 The published WPCL pH dataset only contains these annual minimum and maximum pH data,
140 reported on the NBS pH scale ($\text{pH}_{\text{in situ}}$) and rounded to one decimal place. Water temperature data are
141 also available for each sampling event (http://www.nies.go.jp/igreen/md_down.html). Previous studies
142 have reported negative correlations between seasonal variations in pH and water temperature, mainly
143 because of changes in the dissociation constant; the pH values were lowest in summer and highest in
144 winter, in both the open ocean (e.g. Bates et al. 2014) and coastal waters (e.g., Frankignoulle and
145 Bouquegneau 1990; Byrne et al. 2013; Hagens et al. 2015; Challenger et al. 2016). We therefore
146 assumed that the minimum and maximum pH data coincided with the highest and lowest temperatures,
147 respectively (Fig. 2), and we used these data to calculate pH_{25} in Section 4.2.

148 The monitoring operations were carried out by licensed operators as outlined in the annual plan of
149 the Regional Development Bureau of each prefecture. These specific licensed operators were retained
150 for the duration of the measurement period, which means that the same laboratories were always in
151 charge of collecting the data. This approach helps to prevent systematic errors that might arise both
152 between measurement facilities and over time, and ensures the datasets are accurate.

153

154 2.2 Quality control procedures and assessing the consistency of the WPCL monitoring data

155 We used all the data for fixed sites that had continuous time-series from 1978 to 2009. There were
156 2463 regular and non-regular monitoring sites in 1978 and 2127 sites in 2009. While there were few



157 sites in some prefectures in Hokkaido and Tohoku, the monitoring sites covered almost all the coastline
158 in Japan (Fig. 1).

159 As explained in more detail later in this section, we applied a three-step quality control procedure.
160 We excluded 1) discontinuous time sequences, 2) time sequences that had extreme outliers in each year,
161 and 3) time sequences that included significant random errors and which were only weakly correlated
162 with time sequences at adjacent sites.

163 When we excluded the sites that had discontinuous time sequences of $\text{pH}_{\text{insitu}}$ from 1978 to 2009,
164 1481 sites remained (Fig. 1). We then excluded time sequences with outliers, defined as sites with data
165 points that were more than three standard deviations from the mean for each year. After this step, 1127
166 sites remained (not shown). We calculated the trends in the unbroken continuous time sequences of the
167 minimum and maximum $\text{pH}_{\text{insitu}}$ data at each site with linear regression (Fig. 3), and the slopes of the
168 linear regression were taken as the minimum and maximum $\text{pH}_{\text{insitu}}$ trends (e.g. Fig. 3). The linear
169 regression trends might have been influenced by random errors or variations at different temporal
170 scales in the data for each site. To eliminate the influence of these errors and variations as far as possible,
171 we removed the data that had significant random errors, defined as the time sequences for which the
172 standard deviations of $\text{pH}_{\text{insitu}}$ exceeded the average standard deviation of the $\text{pH}_{\text{insitu}}$ time sequences
173 at the 1127 sites. After this step, 302 sites remained (see Fig. 1b for site locations). As shown in Table
174 2, the correlations between temperature and $\text{pH}_{\text{insitu}}$ at sites that were within 15 km of each other
175 strengthened after steps 2 and 3, which suggests that the reliability of the dataset improved at each step



176 of the quality control. The mutual correlations among the $\text{pH}_{\text{insitu}}$ and temperature measurements at
177 adjacent sites (Table 2), and the correlations between $\text{pH}_{\text{insitu}}$ and TN (Table 3) show that the quality
178 control procedures were effective.

179 For the 302 sites, we calculated the correlations between water temperature (Fig. 4a–b) and $\text{pH}_{\text{insitu}}$
180 (Fig. 4c–d) between pairs of adjacent sites (Fig. 4). At most of the stations, the correlations between
181 the temperatures at the site pairs were relatively strong, which indicates that the temperature followed
182 similar patterns over time at adjacent sites (Fig. 4a–b). The correlations tended to be strong when the
183 sites were close together, but gradually weakened with increasing distance between sites. The patterns
184 in the $\text{pH}_{\text{insitu}}$ and temperature correlations were similar (Fig. 4c–d), which indicates that the $\text{pH}_{\text{insitu}}$
185 and temperature data at adjacent monitoring sites varied in the same way. In other words, the relative
186 ratios of the measurement errors in $\text{pH}_{\text{insitu}}$ and the natural spatio-temporal variations at these
187 monitoring sites were similar to those for temperature. The absolute values of the $\text{pH}_{\text{insitu}}$ correlation
188 coefficients were slightly lower than those for temperature for each corresponding pair of sites (Figs.
189 4 and 5), and might reflect the fact that $\text{pH}_{\text{insitu}}$, but not the water temperature, is subjected to strong
190 forcing by coastal biological processes, which causes short-term variations in $\text{pH}_{\text{insitu}}$. The correlations
191 between the minimum $\text{pH}_{\text{insitu}}$ data were weaker than those for the maximum $\text{pH}_{\text{insitu}}$ data because the
192 degree of biological forcing varied by season and was stronger in summer when $\text{pH}_{\text{insitu}}$ was at a
193 minimum and weaker in the winter when $\text{pH}_{\text{insitu}}$ was at a maximum. Despite the influence of biological
194 processes on $\text{pH}_{\text{insitu}}$, the correlation coefficients remained high and were significant ($r=0.367$, $p<0.05$)



195 at most of the monitoring sites, especially at sites that were less than 5 km apart within the same
196 prefecture; at such sites, $\text{pH}_{\text{insitu}}$ followed similar patterns. In the final step of the quality check
197 procedure (step 3), we removed all the time sequences with weak and insignificant correlations for
198 temperature and $\text{pH}_{\text{insitu}}$ (Figs. 4 and 5). After this final step, 289 sites remained.

199 The monitoring in each prefecture is carried out by different licensed operators, decided by the
200 Regional Development Bureau in each prefecture. Even though all the operators follow the same JIS
201 protocol, manual monitoring can introduce systematic errors into the data. Some adjacent monitoring
202 sites are close to each other but are managed by different operators, such as sites close to the boundaries
203 between Osaka and Hyogo, Hyogo and Okayama (Fig. 6), Kagawa and Okayama (not shown), and
204 Kagawa and Ehime (not shown). The $\text{pH}_{\text{insitu}}$ time sequences for these site pairs were generally similar,
205 even though there were some deviations when compared with the time sequences for adjacent sites
206 within the same prefecture, monitored by the same operator (lines of the same color in Fig. 6). The
207 standard deviations of the $\text{pH}_{\text{insitu}}$ trends between these site pairs close to the boundaries of Osaka and
208 Hyogo, Hyogo and Okayama, Kagawa and Okayama, and Kagawa and Ehime were 0.0014, 0.0012,
209 0.0026, and 0.0017 yr^{-1} , respectively, and were smaller than the acceptable measurement errors of the
210 JIS standard protocols. We can therefore say that the measurements from the different operators in
211 different prefectures were consistent.

212

213 3. Results



214 3.1 Variations in $\text{pH}_{\text{insitu}}$ highlighted by regression analysis

215 The histograms of the calculated $\text{pH}_{\text{insitu}}$ trends (yr^{-1}), for the minimum and maximum $\text{pH}_{\text{insitu}}$ after
216 each quality control step, are shown in Fig. 7. The histogram in Fig. 7a–b shows data of the 1481 sites
217 (discontinuous sites excluded). The data for 1127 sites (i.e., data without outliers from step 2) are
218 shown in Fig. 7c–d, and the data for 289 sites (from step 3) are shown in Fig. 7e–f (Section 2.2). The
219 number of sites decreased at each step of the quality control, but the shapes of the histograms were
220 generally similar for both the minimum and maximum pH trends. The total trends showed overall
221 normal distributions with a negative shift for all the processing level.

222 We detected both positive (basification) and negative (acidification) trends, which contrasts with
223 the findings of other researchers who reported only negative trends (ocean acidification) in the open
224 ocean (Bates et al. 2014; Midorikawa et al. 2010; Olafsson et al. 2009; Wakita et al. 2017). The average
225 (\pm standard deviation) trends for the minimum and maximum $\text{pH}_{\text{insitu}}$ data were -0.0002 ± 0.0061 and
226 $-0.0023 \pm 0.0043 \text{ yr}^{-1}$ for the 1481 sites (Fig. 7a–b), and -0.0005 ± 0.0042 and $-0.0023 \pm 0.0036 \text{ yr}^{-1}$ for
227 the 1127 sites (Fig. 7c–d), respectively. The average trends for the minimum and maximum $\text{pH}_{\text{insitu}}$
228 data for the 289 sites that remained after step 3 were -0.0014 ± 0.0033 and $-0.0024 \pm 0.0042 \text{ yr}^{-1}$,
229 respectively (Fig. 7e–f).

230 The negative trends were relatively weak for the minimum $\text{pH}_{\text{insitu}}$ data and relatively strong for
231 the maximum $\text{pH}_{\text{insitu}}$ data, but there was an overall tendency towards acidification. The trends that we
232 detected for all the processing levels (Fig. 7) are consistent with, and within the errors of, those reported



233 by Midorikawa et al. (2010), who calculated that pH_{25} decreased at rates of $0.0013 \pm 0.0005 \text{ yr}^{-1}$ and
234 $0.0018 \pm 0.0002 \text{ yr}^{-1}$ in summer and winter from 1983 to 2007 along the 137°E line of longitude in the
235 north Pacific.

236 At the 289 sites, there were 204 negative and 86 positive trends for the minimum $\text{pH}_{\text{insitu}}$ data and
237 217 and 72 negative and positive trends for the maximum $\text{pH}_{\text{insitu}}$ data. This shows that for the
238 minimum data, there were acidification and basification trends at 70% and 30% of the monitoring sites,
239 respectively, with values of 75% and 25% for the maximum data, respectively.

240

241 3.2 Local patterns in acidification and basification

242 We examined the $\text{pH}_{\text{insitu}}$ trends for the 289 sites for local patterns in acidification and basification
243 (Section 2.2), and found that the trends seemed to be randomly distributed. For example, the values
244 were different at sites that were less than 50 km apart (Fig. 8). There are many monitoring sites in the
245 Seto Inland Sea and in Western Kyushu. The trends for the minimum and maximum $\text{pH}_{\text{insitu}}$ showed
246 both acidification and basification in the Seto Inland Sea (Fig. 8a–b, 8c–d). In the western part of
247 Kyushu, acidification dominated (Fig. 8a–b, 8c–d) and there were few clusters of basification in
248 $\text{pH}_{\text{insitu}}$ for both the minimum and maximum $\text{pH}_{\text{insitu}}$ data (Fig. 8b, d). Figure 8a (b) and Figure 8c (d)
249 are similar, which suggests that, at most of the sites where we detected acidification and basification,
250 the trend directions were consistent for the minimum and maximum $\text{pH}_{\text{insitu}}$ (Fig. 8a–b, 8c–d).

251 By examining the average minimum and maximum $\text{pH}_{\text{insitu}}$ trends in each prefecture (Fig. 9a–b, d–e,



252 g–h, j–k), we found that, while the average values were slightly different, the trends in the averaged
253 values and the patterns in acidification and basification for both the minimum and maximum $\text{pH}_{\text{insitu}}$
254 were the same from north to south and from west to east. We also found acidification trends in most of
255 the prefectures with at least 17 sampling sites, namely Miyagi, Wakayama, Hyogo, Okayama,
256 Yamaguchi, Tokushima, Kagawa, Ehime, and Nagasaki (Figs. 1a and 9c, f, i, l). The average estimates
257 for the maximum $\text{pH}_{\text{insitu}}$ were larger than those for the minimum $\text{pH}_{\text{insitu}}$ in these prefectures.

258 We found more acidification trends for the minimum $\text{pH}_{\text{insitu}}$ in the southwestern prefectures of
259 Yamaguchi, Kagawa, Ehime, Hyogo, and Nagasaki than in the northeastern prefecture of Miyagi (Fig.
260 9a, d, g, i) (see Fig. 1 for locations). The maximum and minimum $\text{pH}_{\text{insitu}}$ trends indicated basification
261 in Wakayama and Okayama prefectures (Fig. 9c). The trends in Osaka, Hyogo, Okayama, Hiroshima,
262 Yamaguchi, Kagawa, and Ehime prefectures (Fig. 1a) were different from each other, even though they
263 were all located in the same part of the Seto Inland Sea (Fig. 9d–e). The trends in Hiroshima and
264 Okayama, within the Seto Inland Sea, were weaker than those in Hyogo, Yamaguchi, Kagawa, and
265 Ehime, which were outside the sea (Fig. 9d–e). The $\text{pH}_{\text{insitu}}$ trend values indicated relatively strong
266 acidification at -0.0025 yr^{-1} in Niigata in the Japan Sea (Fig. 9j–l) but there were fewer than the
267 threshold of 17 monitoring sites in the prefectures.

268

269 4. Discussion

270 4.1 Statistical evaluation of our estimated overall trends



271 The JIS Z8802 (2011) allows a measurement error of ± 0.07 and this treatment further enhanced the
272 uncertainty of the published data to ± 0.1 . The uncertainty of the slope of the linear regression line (σ_β)
273 is estimated by the following equation (e.g., Luenberger 1969):

$$274 \quad \sigma_\beta = \{ \sigma_y^2 / \sum (x_i - [x])^2 \}^{1/2} \quad (1)$$

275 where σ_y^2 is the theoretical variance in a pH value caused by the measurement error (in this case, $0.1^2 =$
276 0.01); and x_i and $[x]$ represent the year and the year averaged for all data at a station, respectively. In
277 the WPCL dataset, there are generally 32 data points for each station (for every year from 1978 to
278 2009), spaced at consistent intervals. In this case, $\sum (x_i - [x])^2$ becomes 2728 and σ_β becomes 0.0020
279 yr^{-1} , which is the threshold of significance for the pH trend. This means that our estimated trends
280 included standard deviations that were less than 0.0020 yr^{-1} , and, if there were no trends, a histogram
281 of pH trends should have a normal distribution with an average and standard deviation (σ_β) of 0.0000
282 and 0.0020 yr^{-1} , respectively (Fig. 7). The average trend in the maximum $\text{pH}_{\text{insitu}}$, however, shifted
283 from zero in a negative direction at a rate of more than 0.0023 yr^{-1} for all three scenarios. This result
284 implies that averaged over the whole country, the Japanese coast was acidified in winter to a degree
285 that could be detected from the historical WPCL pH data, even with an uncertainty of ± 0.1 . The
286 observed standard deviation for the maximum $\text{pH}_{\text{insitu}}$ was also larger than the expected value of 0.0020
287 yr^{-1} because of local variations in the pH trends. The average shift in the minimum $\text{pH}_{\text{insitu}}$ data was
288 smaller than 0.0020 yr^{-1} , but all three scenarios showed negative shifts in the average minimum $\text{pH}_{\text{insitu}}$
289 value (Fig. 7a, c, e).



290 We used Welch's t test to assess the direction of the average minimum and maximum $\text{pH}_{\text{insitu}}$ trends.
291 For our null hypothesis, we assumed that the population of the trends with an average of -0.0014 yr^{-1}
292 (-0.0024 yr^{-1}) and a standard deviation of 0.0033 yr^{-1} (0.0042 yr^{-1}) was sampled from a population
293 with an average trend of 0.0000 yr^{-1} and a standard deviation of 0.0020 yr^{-1} . When the sample size
294 was 289, the t -values and the degrees of freedom were 8.7 (6.2) and 412.2 (474.4), respectively. Since
295 the p value was less than 0.001, the null hypothesis was rejected. Welch's t test confirmed that the
296 average trends for both the minimum and maximum $\text{pH}_{\text{insitu}}$ data were negative.

297

298 4.2 Possible influences on the $\text{pH}_{\text{insitu}}$ trends in coastal waters

299 To facilitate our discussion of the factors that influenced the $\text{pH}_{\text{insitu}}$ trends, we used the conceptual
300 models of acidification and basification in coastal waters of Sunda and Cai (2012) and Duarte et al.
301 (2013), as follows:

$$302 \quad \text{pH}_{\text{insitu}} = \text{Function} (D (T), \text{DIC} (\text{Air CO}_2, B (T, N)), \text{Alk}(S)) \quad (2)$$

303 The $\text{pH}_{\text{insitu}}$ varies with the ambient temperature (T) on seasonal, inter-annual, and decadal time scales
304 mainly because of changes in the water dissociation constant (D). Changes in dissolved inorganic
305 carbon (DIC), alkalinity (Alk), and salinity (S) also affect the $\text{pH}_{\text{insitu}}$ trends. The solubility pump,
306 which is controlled mainly by the atmospheric CO_2 concentration (Air CO_2), affects DIC , and ocean
307 acidification occurs when the Air CO_2 increases. Dissolved organic carbon can also be affected by
308 biological processes (B) that depend on the ambient temperature (T) and the nutrient loading (N).



309 There are contrasting relationships between DIC and N in heterotrophic and autotrophic oceans.

310 Because of the balance between primary productivity and respiration in heterotrophic (autotrophic)

311 oceans, the DIC increases as N increases (decreases), causing acidification, but decreases as N

312 decreases (increases), causing basification. Alkalinity (Alk) generally varies with salinity (S) in coastal

313 oceans and might also affect the $\text{pH}_{\text{insitu}}$ trend.

314 The DIC process (Air CO_2) of ocean acidification in equation 2 generally occurred at all monitoring

315 sites when the Air CO_2 concentrations were horizontally uniform, resulting in overall negative trends

316 in minimum and maximum $\text{pH}_{\text{insitu}}$. D (T) also has an overall trend of warming in Japan coastal area,

317 and hence made some affections to the observed $\text{pH}_{\text{insitu}}$ trend. We will discuss about this effect in

318 the next [chapter](#).

319 On the other hand, both DIC (B (T, N)) and Alk (S) are difficult to have general trends that covered

320 all monitoring sites, because factors that control these variables (e.g., salinity of coastal water and

321 terrestrial nutrient loading) have no mutual trends all over the Japan coast. WPCL data contains stations

322 of both autotrophic and heterotrophic oceans, and this condition further obscure [affection](#) of DIC (B

323 (T, N)) to overall $\text{pH}_{\text{insitu}}$ trend, as the same trend of B (T, N) leads opposite trends of DIC (B (T, N)

324 between autotrophic and heterotrophic ocean. Wide-varying nature of D(T), DIC (B (T, N)), and

325 Alk(S) depending on the season and region, however, might have caused the seasonal/regional

326 differences of $\text{pH}_{\text{insitu}}$ trends among stations, contributing relatively large standard deviations of both

327 the minimum and maximum $\text{pH}_{\text{insitu}}$ trends (Figures 7).



328

329 4.2.1 Seasonal variations in $\text{pH}_{\text{insitu}}$ trends330 Our estimates of the average $\text{pH}_{\text{insitu}}$ trends show that there was a difference of $0.0010\text{--}0.0020 \text{ yr}^{-1}$ 331 between the winter and summer trends (Section 3.1, Fig. 7e–f). Our analysis was based on the $\text{pH}_{\text{insitu}}$

332 data, so the difference between the trends might reflect long-term changes in water temperature that

333 affected the dissociation constant (process D in equation 2) or changes in the coastal carbon cycle

334 (including absorption of anthropogenic carbon by the solubility pump, represented by DIC in equation

335 2).

336 To evaluate the direct thermal effects related to process D in equation 2, we estimated the pH values

337 normalized to 25°C (pH_{25}), assuming that the minimum (maximum) $\text{pH}_{\text{insitu}}$ and highest (lowest)

338 temperature and other parameters were measured at the same time. By assuming the other parameters

339 that affected the pH calculation in the CO2sys software (Lewis and Wallace 1998, csys.m), such as

340 salinity, DIC, and alkalinity, did not change (these parameters are not measured as part of the WPCL

341 program), we used the method of Lui and Chen (2017) to calculate the pH_{25} , as follows:

342
$$\text{pH}_{25} = -\text{pH}_{\text{insitu}} + a_1(T - 25^\circ\text{C}), \quad (3)$$

343 where a_1 is set to -0.015 and T is the observed temperature.344 The distributions of the trends in pH_{25} after applying equation 3 are shown in Fig. 10. The minimum345 and maximum pH_{25} data were normally distributed, meaning that the distributions of the $\text{pH}_{\text{insitu}}$ trends346 were maintained after applying equation 3 (Fig. 7e, f). The averages (\pm standard deviations) of the



347 minimum and maximum pH_{25} trends were -0.0010 ± 0.0032 and $-0.0014 \pm 0.0041 \text{ yr}^{-1}$, respectively, so
348 the average for the minimum and maximum pH_{25} still showed acidification, but the trends were slightly
349 weaker than those for the minimum and maximum $\text{pH}_{\text{insitu}}$ (-0.001 yr^{-1} less) (Fig. 7e–f).

350 The pH_{25} and $\text{pH}_{\text{insitu}}$ trends from north to south and from west to east were similar among the
351 prefectures (Fig. 11), except in Miyagi and Tokushima. The trends in the minimum $\text{pH}_{\text{insitu}}$ and summer
352 pH_{25} were quite similar, but the minimum and maximum $\text{pH}_{\text{insitu}}$ trends tended to be more negative (by
353 about -0.0010 yr^{-1}) than the corresponding pH_{25} trends, especially in Wakayama, Hiroshima, Kagawa,
354 and Ehime, which met the threshold number of sampling sites.

355 The average highest temperatures observed at the minimum $\text{pH}_{\text{insitu}}$ were close to 25°C in the regions
356 south of Chiba prefecture (Figs. 1 and 12a–d), so we were not able to remove the thermal effects from
357 the minimum pH_{25} in the southern prefectures. In contrast, the maximum $\text{pH}_{\text{insitu}}$ values were observed
358 at temperatures that were more than 10°C lower than 25°C , so we were able to normalize the winter
359 data. We estimated the temperature trends from the highest and lowest temperatures at the 289 sites
360 that remained after quality control step 3. The trends in the highest and lowest temperatures generally
361 indicated warming, with an average and standard deviation of 0.021 ± 0.040 and $0.047 \pm 0.036 \text{ }^\circ\text{C yr}^{-1}$,
362 respectively (Fig. 13). Estimations from the CO2sys software indicate that these warming trends
363 influenced the pH values and were related to the changes of -0.0004 and -0.0010 yr^{-1} in the pH trends
364 in summer and winter, respectively (Fig. 7e–f and 10a–b). We estimated that the $\text{pH}_{\text{insitu}}$ would change
365 from 8.0150 to 8.0147 in summer and from 8.2560 to 8.2565 in winter, for temperature changes from



366 25.00°C to 25.02°C, and from 10.00°C to 10.04°C, respectively, for a salinity of 34, DIC of 1900
367 millimole m⁻³, and alkalinity of 2200 millimole m⁻³. The differences between the pH_{insitu} and the
368 corresponding pH₂₅ trends in summer (0.0004 yr⁻¹) and winter (-0.0010 yr⁻¹) can be partly explained
369 by the difference between the decrease in the pH trends in summer (-0.0003 yr⁻¹) and winter (-0.0005
370 yr⁻¹) (Fig. 7e–f) arising from thermal effects.

371

372 4.2.2 Regional differences in pH_{insitu} trends

373 We found regional differences in pH_{insitu} values (e.g. Fig. 6) and pH_{insitu} trends (Figs. 8–9). The
374 negative pH_{insitu} trends (acidification) were more significant in southwestern Japan than in northeastern
375 Japan, especially for the minimum pH_{insitu} data (Fig. 9 and Section 3.2). The JMA (2008, 2018)
376 reported that over the past 100 years, the increase in water temperature in western Japan was ~1.30°C
377 greater than ~~that~~ in northeastern Japan.

378 We used the CO2sys ~~software~~ (Lewis and Wallace 1998) to predict how pH_{insitu} would change under
379 a temperature difference of 0.01 °C yr⁻¹ between the northeastern and southwestern areas, and found
380 that pH decreased by 0.0002 (0.0002) yr⁻¹ when the temperature changed from 10.00°C to 10.01°C
381 (25.0°C to 25.01°C), assuming a salinity of 34, DIC of 1900 millimol/m³, and alkalinity of 2200
382 millimol/m³. The contrasting trends in the northeast and southwest can be also partly explained by the
383 difference in warming trends (process D in equation 2).

384 Regional differences in pH were observed in the northern Gulf of Mexico and the East China Sea



385 (Cai et al. 2011) at the basin scale. Yamamoto-Kawai et al. (2015) detected regional differences in the
386 aragonite saturation rate (Ω_{ar}) of an ocean acidification index, but not in pH_{insitu} , in Tokyo Bay. Cai et
387 al. (2011) reported that regional differences in pH_{insitu} observed in their surveys were caused by human-
388 related inputs of nutrients to coastal waters; i.e., eutrophication (represented by the DIC process in
389 equation 2). Sunda and Cai (2012) used biogeochemical simulations to examine the complex
390 interactions between acidification that resulted from respiratory CO_2 inputs and from increasing
391 atmospheric CO_2 . With their model, which focused on coastal areas, they predicted that these CO_2
392 inputs caused pH_{insitu} values to decrease by between 0.1250 and 1.1000 units because of eutrophication.
393 Both Cai et al. (2011) and Sunda and Cai (2012) considered heterotrophic subsurface waters. Spatial
394 variations in nutrient loadings in autotrophic waters also cause pH_{insitu} trends to vary, although in the
395 opposite direction (Borges and Gypens 2010), and eutrophication can result in basification (Duarte et
396 al. 2013).

397 As well as the effect of changes in the dissociation constant, the summer pH_{insitu} is affected by
398 ocean uptake of CO_2 (process DIC; Bates et al. 2012; Bates 2014) through long-term changes in
399 biological activity (Cai et al. 2011; Sunda and Cai 2012; Duarte et al. 2013; Yamamoto-Kawai et al.
400 2015). The responses of pH_{insitu} to changes in marine productivity are, however, complicated.

401 Previous studies have reported that nutrient loadings in Japan have decreased over recent decades
402 (e.g., Yamamoto-Kawai et al. 2015; Kamohara et al. 2018; Nakai et al. 2018), with variable effects on
403 summer pH_{insitu} in coastal waters. TN was monitored for a shorter period than pH_{insitu} (1995 to 2009).



404 We assumed that the TN was mainly dissolved inorganic nitrogen, and determined the correlations
405 between TN and the minimum and maximum $\text{pH}_{\text{insitu}}$ data (Fig. 14). There were significant negative
406 correlations between TN and minimum (-0.03) and maximum (-0.29) $\text{pH}_{\text{insitu}}$. These correlations
407 imply that the conditions in most of the monitoring areas of the WPCL programs were heterotrophic.
408 There is little evidence of basification, even in coastal waters, but the heterotrophic coastal waters
409 monitored by the WPCL programs might have been oligotrophic. While some sites might have been
410 dominated by heterotrophs, others might have been affected by autotrophs, causing the dominant
411 processes in the pH trends to vary between sites, depending on the area.

412 Nakai et al. (2018) reported that nutrient loadings have decreased in the most parts of the Seto Inland
413 Sea from 1981 to 2010, but several areas remain eutrophic. Because of geographical variations in
414 nutrient loadings and the uneven distribution of autotrophic and heterotrophic water areas, there are
415 significant spatial variations in pH trends in the Seto Inland Sea (Fig. 8). The pH trends in coastal areas
416 of western Kyushu, where the anthropogenic nutrient loadings are relatively low, therefore reflect the
417 decreases in nutrient discharges, resulting in variations between regions (e.g., Nakai et al. 2018;
418 Yamamoto and Hanazato 2015; Tsuchiya et al., 2018). Several cities in this area have introduced
419 advanced sewage treatment to prevent eutrophication in coastal waters (Nakai et al. 2018; Yamamoto
420 and Hanazato 2015).

421 Variations in coastal alkalinity along with salinity might be related to changes in land use and might
422 affect the trends (process Alk(S) in equation 2). Total alkalinity is not monitored as part of the WPCL



423 program and there are no sites in coastal areas of Japan with continuous data for alkalinity. Taguchi et
424 al. (2009) measured alkalinity in the surface waters of Ise, Tokyo, and Osaka bays between 2007 and
425 2009, and reported that total alkalinity was highly correlated with salinity in each bay. For a
426 temperature, salinity, dissolved carbon, and alkalinity of 25.00 °C, 35, 1900 millimol m⁻³, and 2300
427 millimol m⁻³, respectively, pH_{insitu} (= pH₂₅) was estimated at 8.1416 using the CO2sys software (Lewis
428 and Wallace 1998). By changing the salinity and alkalinity to 34 and 2200 millimol m⁻³, respectively,
429 pH_{insitu} (= pH₂₅) decreased by 0.0081 to 8.0150. This shows that pH could deviate significantly from
430 average trends if the inputs of alkaline compounds are changed; consequently, some of our pH trends
431 could have been affected by changing discharge from different land-use types.

432 Regional differences in pH_{insitu} trends in coastal waters might be caused by ocean pollution. The
433 speciation and bioavailability of heavy metals change in acidic waters, causing an increase in the
434 biotoxicity of the metals (Zeng et al. 2015; Lacoue-Labarthe et al. 2009; Pascal et al. 2010; Cambell
435 et al. 2014). The rates at which marine organisms photosynthesize and respire in ocean waters decrease
436 and increase, respectively, in water polluted with heavy metals and oils (process DIC in equation 2)
437 because of biotoxicity and eutrophication, thereby resulting in acidification (Hing et al. 2011; Huang
438 et al. 2011; Gilde and Pinckney 2012).

439

440 5. Conclusions

441 We estimated the long-term trends in pH_{insitu} in Japanese coastal waters and examined how the



442 trends varied regionally. The long-term $\text{pH}_{\text{insitu}}$ data show highly variable trends, although ocean
443 acidification has generally intensified in Japanese coastal waters. We found that the annual $\text{pH}_{\text{insitu}}$
444 minimum (in summer) and $\text{pH}_{\text{insitu}}$ maximum (in winter) decreased at overall rates of -0.0014 and
445 -0.0024 yr^{-1} , respectively, in Japanese coastal waters, similar to the adjacent open ocean. The seasonal
446 differences in average pH trends might reflect differences in warming trends, and the regional
447 differences in pH trends are partly related to heterotrophic processes associated with nutrient loadings.

448 There were striking spatial variations in the $\text{pH}_{\text{insitu}}$ trends. Correlations among the $\text{pH}_{\text{insitu}}$ time series
449 at different sites revealed that the high variability in the $\text{pH}_{\text{insitu}}$ trends was not caused by analytical
450 errors in the data but reflected the large spatial variability in the physical and chemical characteristics
451 of coastal environments, such as water temperature, nutrient loadings, and autotrophic/heterotrophic
452 conditions. While there was a general tendency towards coastal acidification, there were positive trends
453 in $\text{pH}_{\text{insitu}}$ at 25%–30% of the monitoring sites, indicating basification, which suggests that the coastal
454 environment might not be completely devastated by acidification. If we can manage the coastal
455 environment effectively (e.g., control nutrient loadings and autotrophic/heterotrophic conditions), we
456 might be able to limit, or even reverse, acidification in coastal areas.

457

458 Acknowledgments

459 We thank the scientists, captain, officers, and personnel of the National Institute for Environmental
460 Studies, Regional Development Bureau of the Ministry of Land, Infrastructure, Transport and Tourism,
461 who contributed to this study. We acknowledge financial support from the Sasakawa Peace Foundation



462 of the Ocean Policy Research Institute. We also appreciate discussions with members of the
463 Environmental Variability Prediction and Application Research Group of the Japanese Agency for
464 Marine-Earth Science and Technology. Suggestions by two reviewers helped us to improve an earlier
465 version of the manuscript.

466

467 References

468 Bates, N. R.: Interannual variability of the ocean CO₂ sink in the subtropical gyre of the North Atlantic
469 Ocean over the last 2 decades, *J. Geophys. Res.* 112, C09013, doi:10.1029/2006JC003759, 2007.

470 Bates, N. R.: Multi-decadal uptake of carbon dioxide into subtropical mode waters of the North
471 Atlantic Ocean. *Biogeosciences* 9:2, 649–2, 659, <http://dx.doi.org/10.5194/bg-9-2649-2012>, 2012.

472 Bates, N. R., Astor, Y. M., Church, M. J., Currie, K., Dore, J. E., Gonzalez-Davila, M., Lorenzoni, L.,
473 Muller-Karger, F., Olafsson, J., and Santana-Casiano, J. M.: A time-series view of changing surface
474 ocean chemistry due to ocean uptake of anthropogenic CO₂ and ocean acidification, *Oceanography*,
475 27 (1):126–141, <http://dx.doi.org/10.5670/oceanog.2014.16>, 2014.

476 Bednarsek, N., Tarling, G. A., Bekker, D. C. E., Fielding, S., Jones, E. M., Venables, H. J., Ward, P.,
477 Kuzirian, A., Leze, B., Feely, R. A., and Murphy, E. J.: Extensive dissolution of live pteropods in
478 the Southern Ocean, *Nature Geoscience Letter*, 5, 881–885, doi: 10.1038/NGEO1635, 2012.

479 Bednarsek, N., Feely, R. A., Reum, J. C. P., Peterson, B., Menkel, J., Alin, S. R., and Hales, B.:
480 *Limacina helicina* shell dissolution as an indicator of declining habitat suitability due to ocean
481 acidification in the California Current Ecosystem, *Proc. R. Soc. B*, 281 20140123, doi:



- 482 10.1098/rspb.2014.0123, 2014.
- 483 Borges, A. V. and Gypen, N.: Carbonate chemistry in the coastal zone responds more strongly to
484 eutrophication than to ocean acidification, *Limnology and Oceanography* 55: 346–353, 2010.
- 485 Montagna, R.: Description and quantification of pteropod shell dissolution: a sensitive bioindicator of
486 ocean acidification, *Global Change Biology*, 18, 2378–2388, doi: 10.1111/j.1365–2486.2012.02668,
487 2012.
- 488 Byrne, M., Lamare, M., Winter, D., Dworjanyn, S. A., and Uthicke, S.: The stunting effect of a high
489 CO₂ ocean on calcification and development in the urchin larvae, a synthesis from the tropics to the
490 poles, *Philosophical Transactions of the Royal Society B*, 368, 20120439. Doi:
491 10.1098/rstb.2012.0439, 2013.
- 492 Cai ,W., Hu, X., Huang, W., Murell, M. C., Lehrter, J. C., Lohrenz, S. E., Chou, W., Zhai, W.,
493 Hollibaugh, J. T., Wang, Y., Zhao, P., Guo, X., Gundersen, K., Dai, M., and Gong, G.: Acidification
494 of subsurface coastal waters enhanced by eutrophication, *Nature Geoscience*, 4, 766–700, 2011.
- 495 Campbell, A. L., Mangan, S., Ellis, R. P., and Lewis, C.: Ocean acidification increases copper toxicity
496 to the early life history stages of the polychaete *arenicola marina* in artificial seawater, *Environ. Sci.*
497 *Technol.* 48, 9745–9753, 2014.
- 498 Challener, R. C., Robbins, L. L., and McClintock, J. B.: Variability of the carbonate chemistry in a
499 shallow, seagrass-dominated ecosystem: implications for ocean acidification experiments, *Marine*
500 *and Freshwater Research*, 67, 163-172. Doi:10.1071/MF14219, 2016.



- 501 DOE (United States Department of Energy): Handbook of methods for the analysis of the various
502 parameters of the carbon dioxide system in sea water; ver. 2, edited by A. G. Dickson and C. Goyet,
503 ORNL/CDIAC-74, 1994.
- 504 Dore, J. E., Lukus, R., Sadler, D. W., Church, M. J. and Karl, D. M.: Physical and biogeochemical
505 modulation of ocean acidification in the central North Pacific, *Proc. Natl. Acad. Sci.* 106, 12 235–12
506 240, 2009.
- 507 Doney, S.C., Fabry, V. J., Freely, A., and Kleypas, J. A.: Ocean acidification: The other CO₂ program,
508 *Annu. Rev. Mar. Sci.* 1, 169–192, 2009.
- 509 Duarte, C. M., Hendriks, I. E., Moore, T. S., Olsen, Y. S., Steckbauer, A., Ramajo, L., Carstensen, J.,
510 Trotter, J. A., and McCullough, M.: Is ocean acidification an open ocean syndrome? Understanding
511 anthropogenic impacts in seawater pH, *Estuaries and Coasts* 36, 221-236.doi:10.1007/s12237-013-
512 9594-3, 2013.
- 513 Frankignoulle, M., and Bouquegneau, J. M.: Daily and yearly variations of total inorganic carbon in a
514 productive coastal area, *Estuarine, Coastal and Shelf Science* 30, 79-89, 1990.
- 515 Gattuso, J. P., and Hansson, L.: *Ocean acidification*, Oxford Univ. Press, Oxford, 2011.
- 516 Glide, K., and Pinckney, J. L.: Sublethal effects of crude oil on the community structure of estuarine
517 phytokton, *Estuar. Coasts* 35, 853–861, 2012.
- 518 Gonzalez-Davila, M., Santana-Casiano, J. M., and Gonzalez-Davila, E. F.: Interannual variability of



519 the upper ocean carbon cycle in the northeast Atlantic Ocean, *Geophys. Res. Lett.* 34, L07608,
520 doi:10.1029/2006GL028145, 2007.

521 Hagens, M., Slomp, C. P., Meysman, F. J. R., Seitaj, D., Harlay, J., Borges, A. V., and Middelburg, J.
522 J.: Biogeochemical processes and buffering capacity concurrently affect acidification in a seasonally
523 hypoxic coastal marine basin, *Biogeoscience* 12, 1561-1583. Doi:10.5194/bg-12-1561-2015, 2015.

524 Hing, L. S., Ford, T., Finch, P., Crane, M., and Morritt, D.: Laboratory stimulation of oil-spill effects
525 on marine phytoplankton, *Aquat. Toxicol* 103, 32–37, 2011.

526 Huang, Y. J., Jiang, Z. G., Zeng, J. N., Chen, Q. Z., Zhao, Y. Q., Liao, Y. B., Shou, L., and Xu, X. Q.:
527 The chronic effects of oil pollution on marine phytoplankton in a subtropical bay, China. *Environ.*
528 *Monit. Assess.* 176, 517–530, 2011.

529 Intergovernmental Panel on Climate Change (IPCC): Climate Change 2013: The Physical Science
530 Basis. Contribution of Working Group I to the Fifth Assessment Report of the Intergovernmental
531 Panel on Climate Change, ed. Stocker, T. F., Qin, D., Plattner, Gian-Kasper., Tignor, M. M. B., Allen,
532 S. K., Boschung, J., Nauels, A., Zia Y., Bex, V., Midgley, P. M., 1–1535 pp. Cambridge,
533 UK: Cambridge University Press, Cambridge, United Kingdom and New York, NY, USA, 2013.

534 Japanese Industrial Standard Z8802 : <http://kikakurui.com/z8/Z8802-2011-01.html> (in Japanese), 2011.

535 Japanese Meteorological Agency :

536 http://dl.ndl.go.jp/view/download/digidepo_3011050_po_synthesis.pdf?itemId=info%3Andljp%2F
537 [pid%2F3011050&contentNo=1&alternativeNo=&lang=en](http://dl.ndl.go.jp/view/download/digidepo_3011050_po_synthesis.pdf?itemId=info%3Andljp%2Fpid%2F3011050&contentNo=1&alternativeNo=&lang=en), 2008.



538 Japanese Meteorological Agency :

539 https://www.data.jma.go.jp/kaiyou/data/shindan/a_1/japan_warm/japan_warm.html (in Japanese),

540 2018.

541 Kamohara, S., Takasu, Y., Yuguchi, M., Mima, N., and Yoshunari, A.: Nutrient decrease in Mikawa

542 Bay, Bulletin of Aichi Fisheries Research Institute 23, 30-32. (in Japanese), 2018.

543 Keeling, C. D., and Whorf, T. P.: Atmospheric CO₂ concentration—Manoa Loa Observatory, Hawaii,

544 1958-1997 (revised August 1998), ORNL NDP-001, Oak Ridge Natl. Lab. Oak Ridge, TN, 1998.

545 Lacou-Labarthe, T., Martin, S., Oberhansli, F., Teyssie, J. L., Jeffree, R., Gattuso, J. P., and

546 Bustamante, P.: Effects of increased pCO₂ and temperature on tracer element (Ag, Cd and Zn)

547 bioaccumulation in the eggs of the common cuttlefish, *Sepia officinalis*. Biogeosciences 6, 1–3,

548 2009.

549 Lemasson, A. J., Fletcher, S., Hall-Spence, J. M., and Knights, A. M.: Linking the biological impacts

550 of ocean acidification on oysters to changes in ecosystem services: A review, Journal of Experimental

551 Marine Biology and Ecology, 492, 49–62, 2017.

552 Lewis, E., and Wallace, D. W. R.: Program Developed for CO₂ System Calculations. ORNL/CDIAC-

553 105. Carbon Dioxide Information Analysis Center, Oak Ridge National Laboratory, U.S. Department

554 of Energy, Oak Ridge, Tennessee, 1998.

555 Luenberger, D. G.: Optimization by vector space methods, pp. 1-326, John Wiley & Sons, Inc., New

556 York, N.Y, 1969.



- 557 Lui, H., and Chen, A. C.: Reconciliation of pH_{25} and $\text{pH}_{\text{insitu}}$ acidification rates of the surface oceans:
558 A simple conversion using only in situ temperature, *Limnology and Oceanography* : methods, 15,
559 328-355, doi:1002/lom3.10170, 2017.
- 560 Midorikawa, T., Ishii, M., Sailto, S., Sasano, D., Kosugi, N., Motoi, T., Kamiya, H., Nakadate, A.,
561 Nemoto, K., and Inoue, H.: Decreasing pH trend estimated from 25-yr time series of carbonate
562 parameters in the western North Pacific, *Tellus*, 62B, 649–659, doi:
563 10.1111/j.1600–0889.2010.00474.x, 2010.
- 564 Ministry of the Environment: <http://www.env.go.jp/hourei/05/000140.html> (in Japanese), 2018.
- 565 Nakai, S., Soga, Y., Sekito, S., Umehara, S., Okuda, T., Ohno, M., Nishijima, W., and Asaoka, S.:
566 Historical changes in primary production in the Seto Inland Sea, Japan, after implementing
567 regulations to control the pollutant loads, *Water Policy* wp2018093. Doi:10.2166/wp.2018.093, 2018.
- 568 National Institute for Environmental Studies :
569 https://www.nies.go.jp/igreen/explain/water/content_w.html (in Japanese), 2018.
- 570 Olafsson, J., Olafsdottir, S. R., Benoit-Cattin, A., Danielsen, M., Arnarson, T. S., and Takahashi, T.:
571 Rate of Iceland Sea acidification from time series measurements, *Biogeosciences* 6:2, 661–2, 668,
572 <http://dx.doi.org/10.5194/bg-6-2661-2009>, 2009.
- 573 Pascal, P. Y., Fleeger, J. W., Galvez, F., and Carman, K. R.: The toxicological interaction between ocean
574 acidity and metals in coastal meiobenthic copepods, *Mar. Pollut. Bull*, 60, 2201–2208, 2010.
- 575 Sarmiento, J. L., and Gruber, N.: *Ocean Biogeochemical dynamics*, pp. 1-503, Princeton Univ. Press,



- 576 Princeton, New Jersey; Oxfordshire, United Kingdom, 2006.
- 577 Sunda, W. G., and Cai, W. J.: Eutrophication induced CO₂-acidification of subsurface coastal waters:
578 interactive effects of temperature, salinity, and atmospheric pCO₂, *Environ. Sci. Technol.* 46,
579 10651–10659, 2012.
- 580 Taguchi, F., Fujiwara, T., Yamada, Y., Fujita, K., and Sugiyama, M.: Alkalinity in coastal seas around
581 Japan, *Bulletin on coastal oceanography*, Vol.47, No.1, 71–75, 2009.
- 582 Yamamoto-Kawai, M., Kawamura, N., Ono, T., Kosugi, N., Kubo, A., Ishii, M., and Kanda, J.: Calcium
583 carbonate saturation and ocean acidification in Tokyo Bay, Japan, *J. Oceanogr.* 71:427–439, doi
584 10.1007/s10872-015-0302-8, 2015.
- 585 Tsuchiya, K., Ehara, M., Yasunaga, Y., Nakagawa, Y., Hirahara, M., Kishi, M., Mizubayashi, K.,
586 Kuwahara, V. S., and Toda, T.: Seasonal and Spatial Variation of Nutrients in the Coastal Waters
587 of the Northern Goto Islands, Japan, *Bulletin on coastal oceanography*, 55, 125-138. (in
588 *Japanese*), 2018.
- 589 Yamamoto, T., and Hanazato, T.: Eutrophication problems of oceans and lakes, -fishes cannot live in
590 clean water, pp. 1–208, ChijinShokan Co. Ltd, ISBN978-4-8052-0885-4, (in Japanese), 2015.
- 591 Yara, Y., Vogt, M., Fujii, M., Yamano, H., Hauri, C., Steinacher, M., Gruber, N. and Yamano, Y. : Ocean
592 acidification limits temperature-induced poleward expansion of coral habitats around Japan,
593 *Biogeosciences*, 9, 4955–4968, doi : 10.5194/bg-9-4955-2012, 2012.
- 594 Zeng, X., Chen, X., and Zhuang, J.: The positive relationship between ocean acidification and pollution,



595 Mar. Poll. Bull, 91, 14–21, 2015.

596 Wakita, M., Nagano, A., Fujiki, T., and Watanabe, S.: Slow acidification of the winter mixed layer in

597 the subarctic western North Pacific, *J. Geophys. Res. Oceans*, 122, 6923–6935,

598 doi:10.1002/2017JC013002, 2017.

599



600 Figure captions

601

602 Fig. 1 Coastal maps and monitoring sites in Japan. Red points in (a) indicate the fixed sites ($n = 1481$)
603 monitored by the Regional Development Bureau of the Ministry of Land, Infrastructure, Transport,
604 and Tourism, and the Ministry of the Environment (Japan) under the WCPL monitoring program. (b)
605 Monitoring sites that met the strictest criterion ($n = 302$).

606

607 Fig. 2 Distributions of the monthly number of data points (N) for (a) maximum and (b) minimum
608 temperatures collected in each prefecture from the 302 most reliable monitoring sites.

609

610 Fig. 3 Examples of (a) acidification (Kahoku Coast in Ishikawa) and (b) basification (Funakoshi Bay
611 in Iwate) trends at monitoring sites. Red and blue colors indicate the annual minimum and maximum
612 $\text{pH}_{\text{insitu}}$ data and their trends, respectively.

613

614 Fig. 4 Correlations of water temperature and $\text{pH}_{\text{insitu}}$ at adjacent monitoring sites in the same prefecture.
615 Thin lines denote significant correlations ($r = 0.12$, degrees of freedom = 283).

616

617 Fig. 5 Scatter plots of correlation coefficients for water temperature and $\text{pH}_{\text{insitu}}$ at adjacent monitoring
618 sites in the same prefecture. Fig. 5a shows the highest temperature and minimum $\text{pH}_{\text{insitu}}$ data and Fig.



619 5b shows the lowest temperature and maximum $\text{pH}_{\text{insitu}}$ data.

620

621 Fig. 6 Examples of time-series for annual minimum and maximum $\text{pH}_{\text{insitu}}$ data at adjacent monitoring
622 sites close to the boundaries between (a) Osaka and Hyogo and (b) Kagawa and Ehime. Lines of the
623 same color indicate data collected at the same site. Site locations are included to the right of each
624 panel, with the text color corresponding to the colors in each panel.

625

626 Fig. 7 Histogram of pH trends, represented by $\Delta\text{pH}_{\text{insitu}}$, showing the slopes of the linear regression
627 lines for the annual minimum (left) and maximum (right) $\text{pH}_{\text{insitu}}$ data at each monitoring site. The
628 histograms in (a, b), (c, d), and (e, f) show three scenarios: (a, b) all 1481 available sites with
629 continuous records before quality control, (c, d) 1127 sites without outliers, and (e, f) 289 sites that
630 meet the strictest criterion.

631

632 Fig. 8 Distributions of long-term trends in $\text{pH}_{\text{insitu}}$ ($\Delta\text{pH}_{\text{insitu}}/\text{yr}$) in Japanese coastal waters. The colors
633 indicate the ranges of acidification (a, c) and basification (b, d). (a, b) and (c, d) are linked to the data
634 used in Figs. 7e and 7f, respectively.

635

636 Fig. 9 (a–b, d–e, g–h, j–k) Average minimum and maximum $\text{pH}_{\text{insitu}}$ trends ($\Delta\text{pH}_{\text{insitu}}/\text{yr}$) in each
637 prefecture. These figures show each side of the Pacific (a–b), the Seto Inland Sea (d–e), the East



638 China Sea (g–h), and the Japan Sea (j–k). The prefecture names are arranged vertically from eastern
639 (northern) to western (southern) areas. Black and red shading indicate one standard deviation from
640 the average. (c, f, i, l) Number of monitoring sites in each prefecture. The thin dashed line is the
641 threshold value of 17 (i.e., the average number of monitoring sites in all prefectures). The prefectures
642 that meet the threshold are indicated in purple. The figure is based on the results shown in Figs. 7 (e,
643 f) and 8.

644

645 Fig. 10 Same as Fig. 7, but showing the pH_{25} trends at 289 sites (selected by quality control step 3).

646 The value of pH_{25} was estimated using the method of Lui and Chen (2017).

647

648 Fig. 11 (a–b, d–e, g–h, j–k) Same as Fig. 9, but showing the average estimated minimum and
649 maximum pH_{25} trends ($\Delta\text{pH}_{25}/\text{yr}$) for each prefecture. Red lines and points indicate the average
650 minimum and maximum $\text{pH}_{\text{insitu}}$ trends shown in Fig. 9.

651

652 Fig. 12 Average highest and lowest temperatures observed for the minimum and maximum $\text{pH}_{\text{insitu}}$ data
653 for each prefecture. The blue and red lines and shading indicate the average and one standard
654 deviation from the average, respectively. The prefectures that met the threshold of 17 are shown in
655 purple, as in Figs. 9 (c–l) and 11 (c–l).

656



657 Fig. 13 Same as Fig. 7, but showing the highest and lowest temperature trends at 289 sites (selected
658 by quality control step 3).

659

660 Fig. 14 Correlation between trends in total nitrogen (TN) and trends in (a) minimum and (b) maximum
661 $\text{pH}_{\text{insitu}}$. The correlation coefficients are -0.30 and -0.29 for the minimum and maximum $\text{pH}_{\text{insitu}}$,
662 respectively (significance level of 0.05, $r = 0.128$; degrees of freedom = 236).

663

664 Table 1 Number of samples (N) collected at each of the 1481 monitoring sites each year.

665

666 Table 2 Average mutual correlation coefficients among water temperature and $\text{pH}_{\text{insitu}}$ measurements at
667 adjacent monitoring sites in the same prefecture. The averages were calculated from the data for the
668 highest and lowest temperature, and minimum and maximum $\text{pH}_{\text{insitu}}$ within 15 km for the three
669 criteria. We refined the sites using three quality control steps, yielding 1481 (step 1), 1127 (step 2),
670 and 302 (step 3) sites.

671

672 Table 3 Average correlation coefficients of minimum and maximum $\text{pH}_{\text{insitu}}$ trends with total inorganic
673 nitrogen (TN) trends. The degrees of freedom in steps 1 and 2 are the same values because TN data
674 are not necessarily measured at all $\text{pH}_{\text{insitu}}$ monitoring sites and the sampling numbers of monitoring
675 sites for steps 1 and 2 are the same.

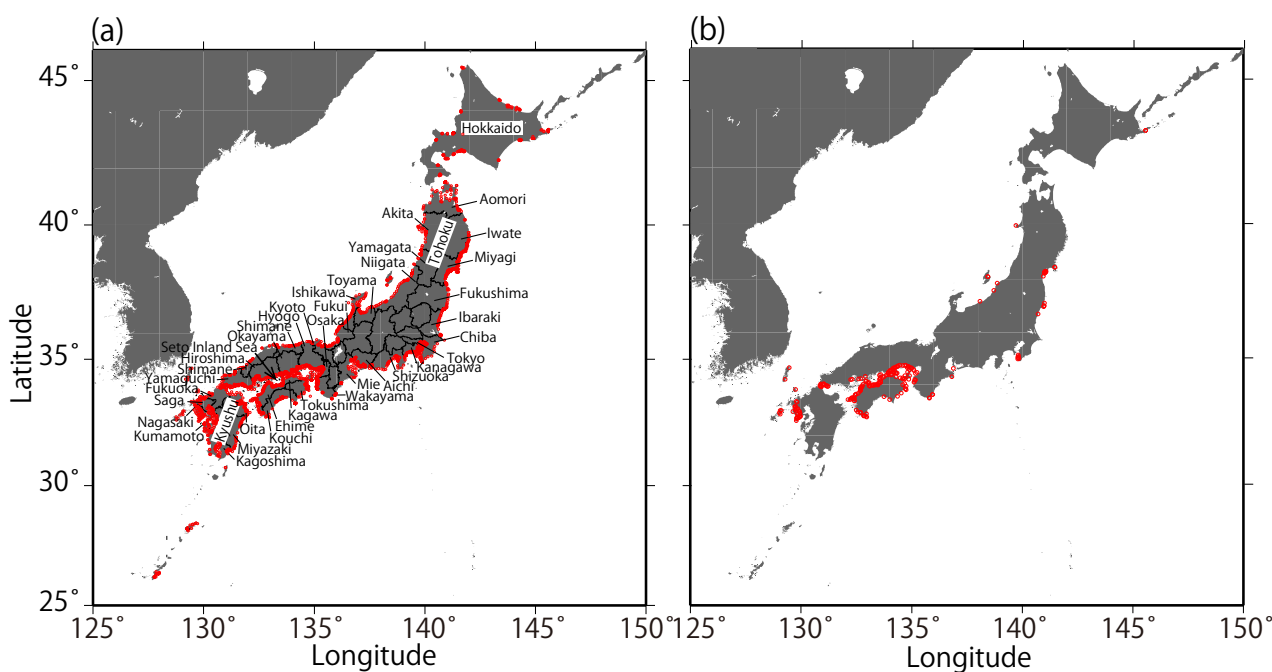


Fig. 1 Coastal maps and monitoring sites in Japan. Red points in (a) indicate the fixed sites ($n = 1481$) monitored by the Regional Development Bureau of the Ministry of Land, Infrastructure, Transport, and Tourism, and the Ministry of the Environment (Japan) under the WCPL monitoring program. (b) Monitoring sites that met the strictest criterion ($n = 302$).

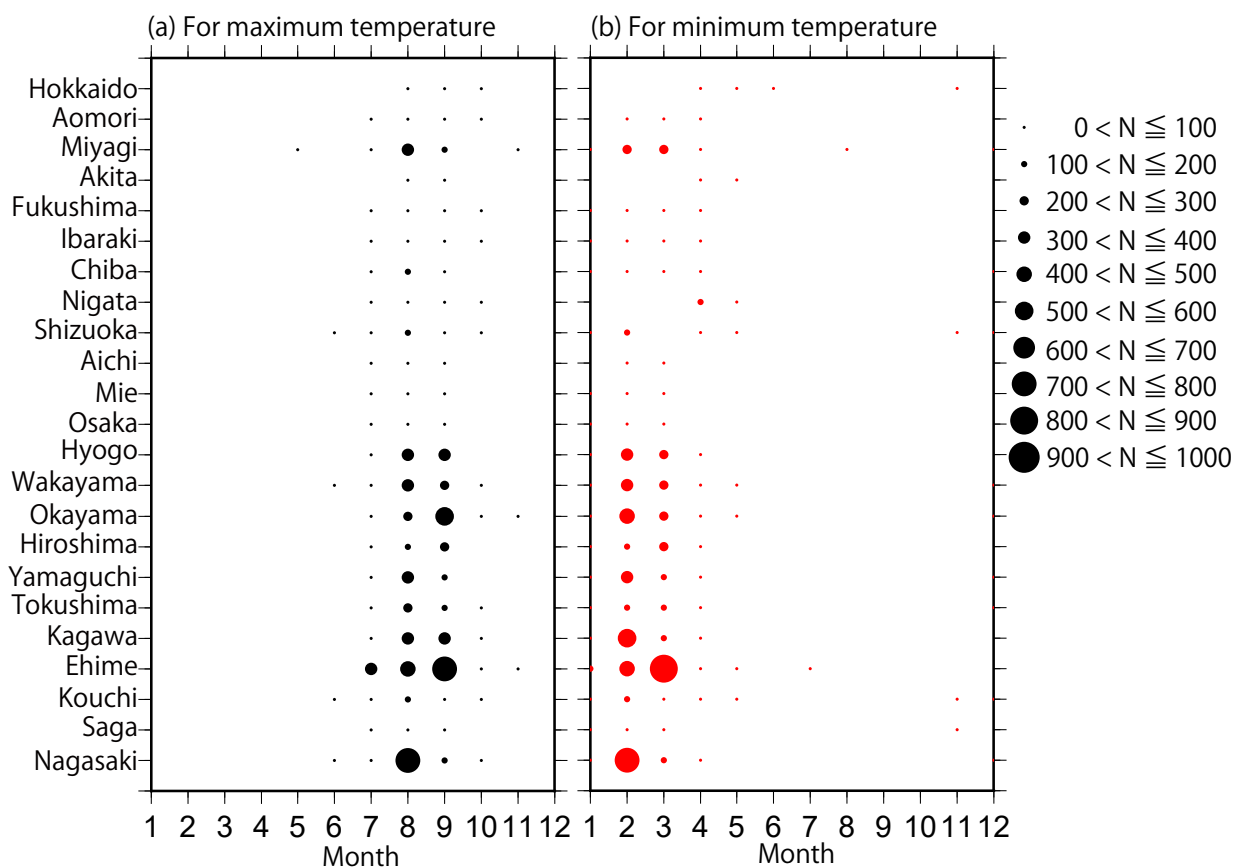


Fig. 2 Distributions of the monthly number of data points (N) for (a) maximum and (b) minimum temperatures collected in each prefecture from the 302 most reliable monitoring sites.

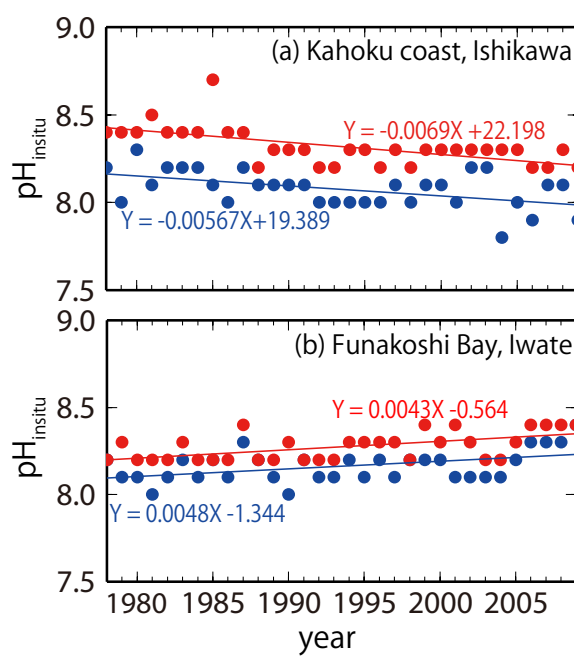


Fig. 3 Examples of (a) acidification (Kahoku Coast in Ishikawa) and (b) basification (Funakoshi Bay in Iwate) trends at monitoring sites. Red and blue colors indicate the annual minimum and maximum pH_{insitu} data and their trends, respectively.

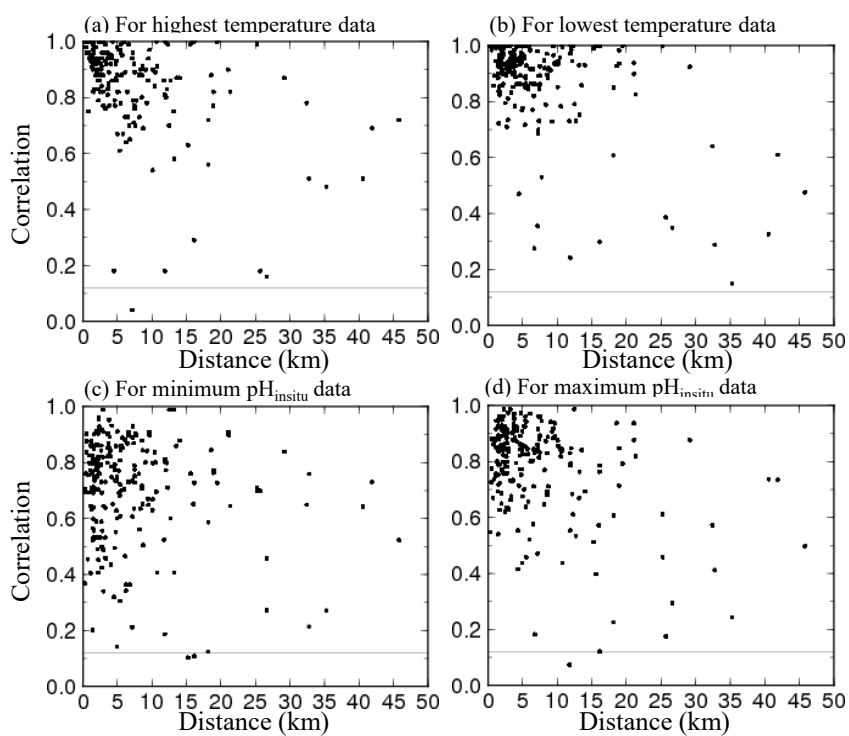


Fig. 4 Correlations of water temperature and $\text{pH}_{\text{in situ}}$ at adjacent monitoring sites in the same prefecture. Thin lines denote significant correlations ($r = 0.12$, degrees of freedom = 283).

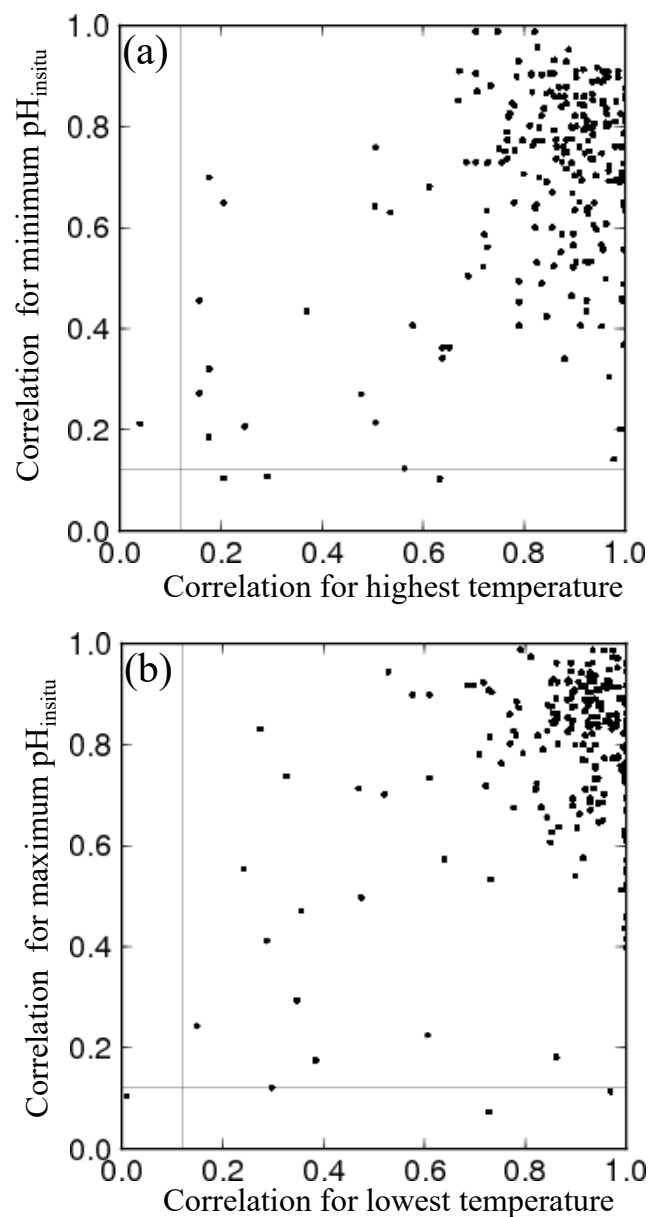


Fig. 5 Scatter plots of correlation coefficients for water temperature and $\text{pH}_{\text{in situ}}$ at adjacent monitoring sites in the same prefecture. Fig. 5a is for the highest temperature and the minimum $\text{pH}_{\text{in situ}}$ data and Fig. 5b for the lowest temperature and the maximum $\text{pH}_{\text{in situ}}$ data, respectively.

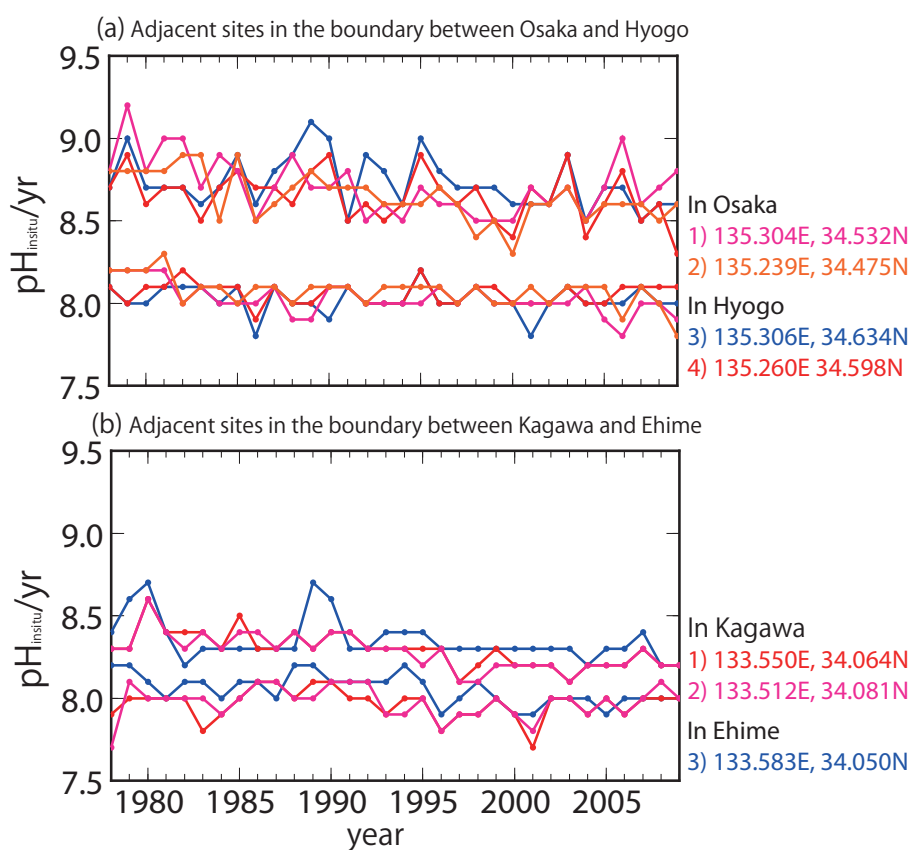


Fig. 6 Examples of time-series for annual minimum and maximum $\text{pH}_{\text{in situ}}$ data at adjacent monitoring sites close to the boundaries between (a) Osaka and Hyogo and (b) Kagawa and Ehime. Lines of the same color indicate data collected at the same site. Site locations are included to the right of each panel, with the text color corresponding to the colors in each panel.

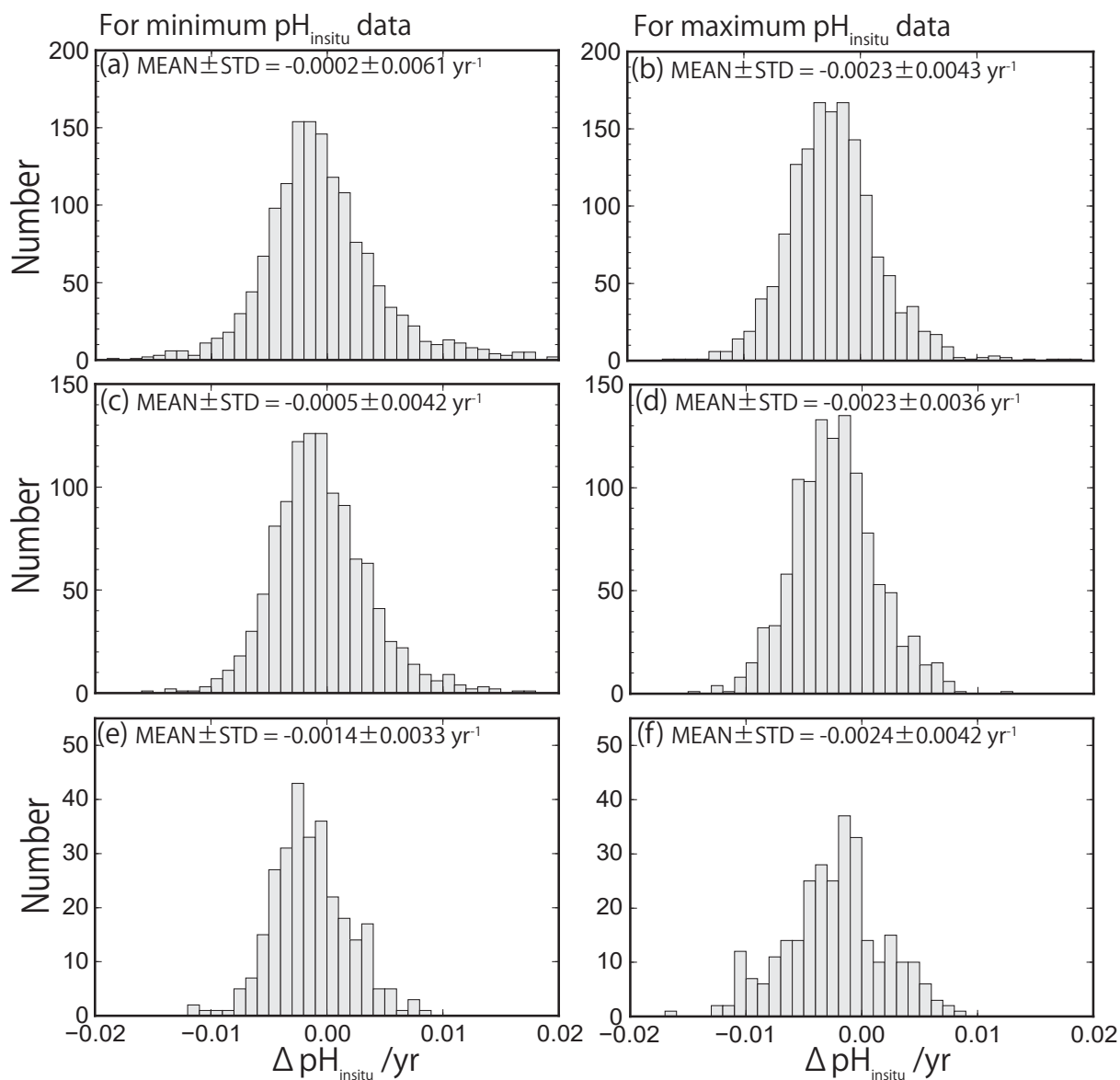


Fig. 7 Histogram of pH trends, represented by $\Delta \text{pH}_{\text{insitu}}$, showing the slopes of the linear regression lines for the annual minimum (left) and maximum (right) $\text{pH}_{\text{insitu}}$ data at each monitoring site. The histograms in (a, b), (c, d), and (e, f) show three scenarios: (a, b) all 1481 available sites with continuous records before quality control, (c, d) 1127 sites without outliers, and (e, f) 289 sites that meet the strictest criterion.

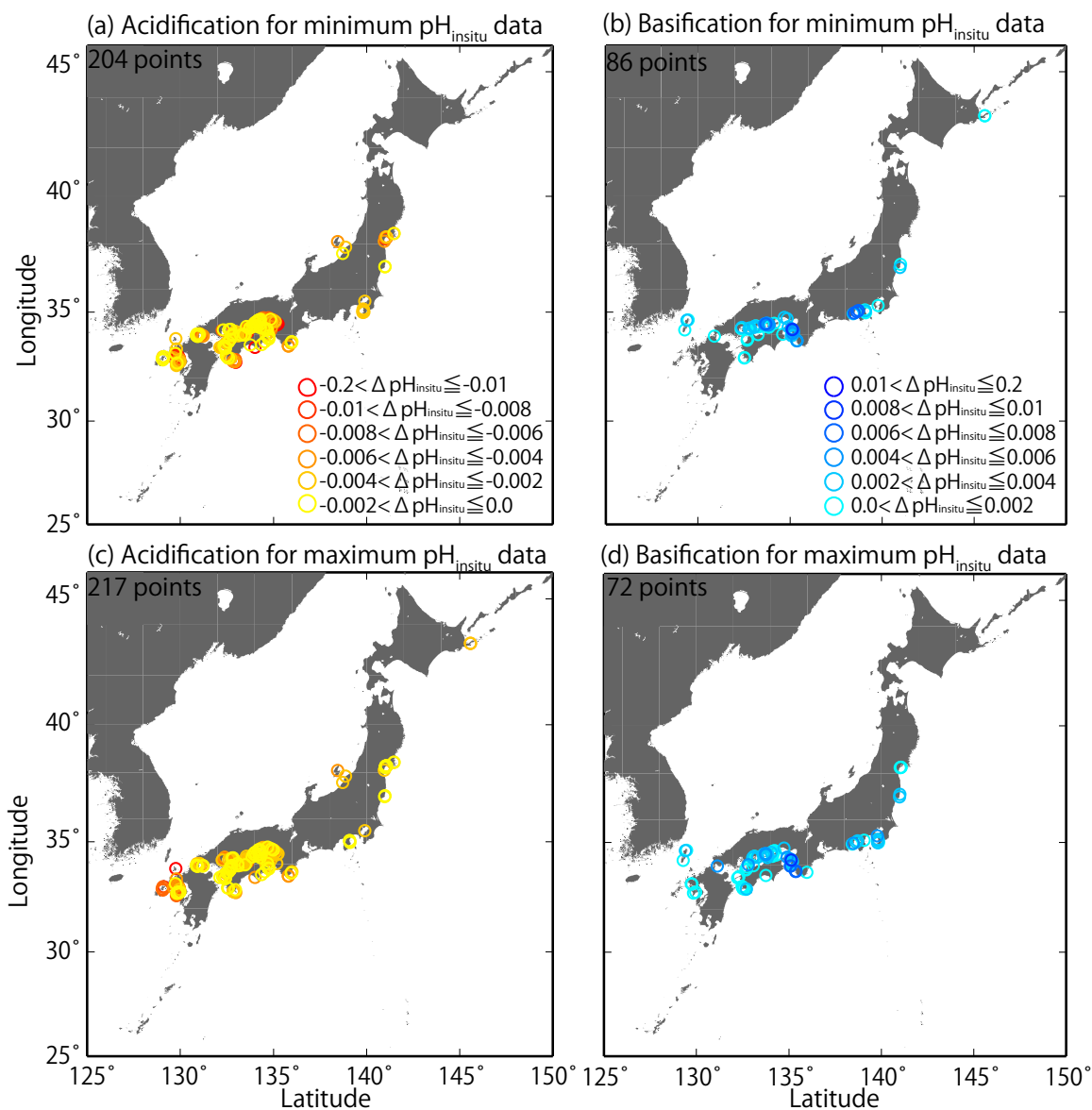


Fig. 8 Distributions of long-term trends in $\text{pH}_{\text{in situ}}$ ($\Delta \text{pH}_{\text{in situ}}/\text{yr}$) in Japanese coastal waters. The colors indicate the ranges of acidification (a, c) and basification (b, d). (a, b) and (c, d) are linked to the data used in Figs. 7e and 7f, respectively.

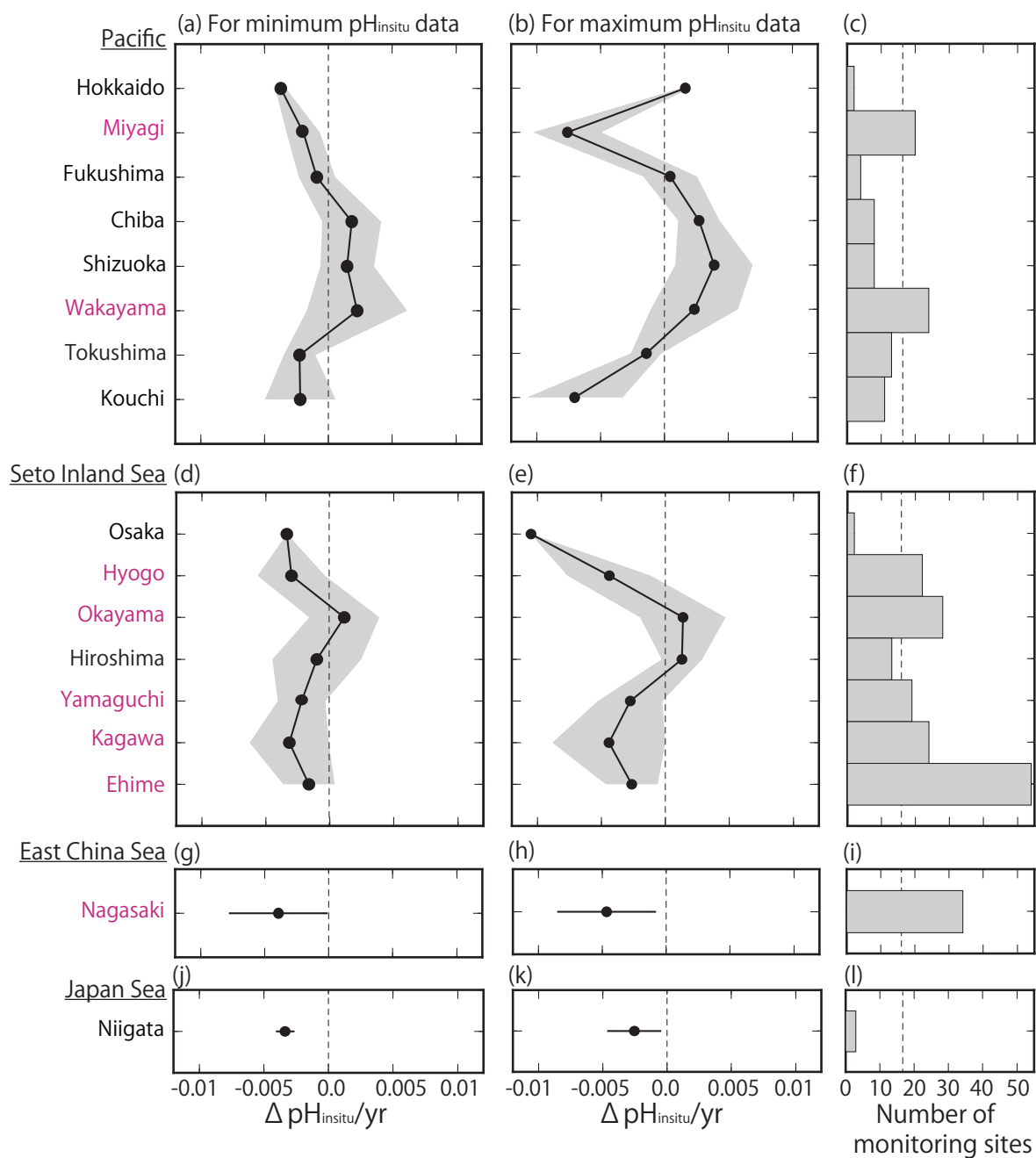


Fig. 9 (a–b, d–e, g–h, j–k) Average minimum and maximum $\text{pH}_{\text{insitu}}$ trends ($\Delta\text{pH}_{\text{insitu}}/\text{yr}$) in each prefecture. These figures show each side of the Pacific (a–b), the Seto Inland Sea (d–e), the East China Sea (g–h), and the Japan Sea (j–k). The prefecture names are arranged vertically from eastern (northern) to western (southern) areas. Black and red shading indicate one standard deviation from the average. (c, f, i, l) Number of monitoring sites in each prefecture. The thin dashed line is the threshold value of 17 (i.e., the average number of monitoring sites in all prefectures). The prefectures that meet the threshold are indicated in purple. The figure is based on the results shown in Figs. 7 (e, f) and 8.

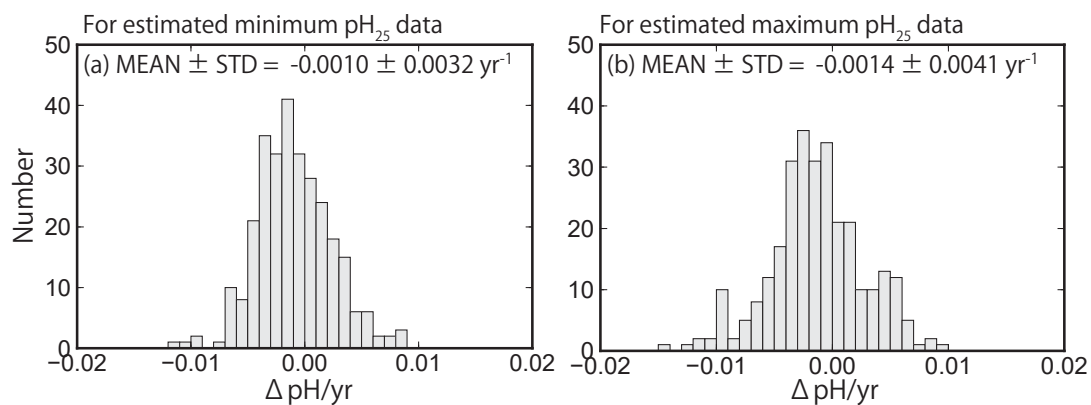


Fig. 10 Same as Fig. 7, but showing the pH_{25} trends at 289 sites (selected by quality control step 3). The value of pH_{25} was estimated using the method of Lui and Chen (2017).

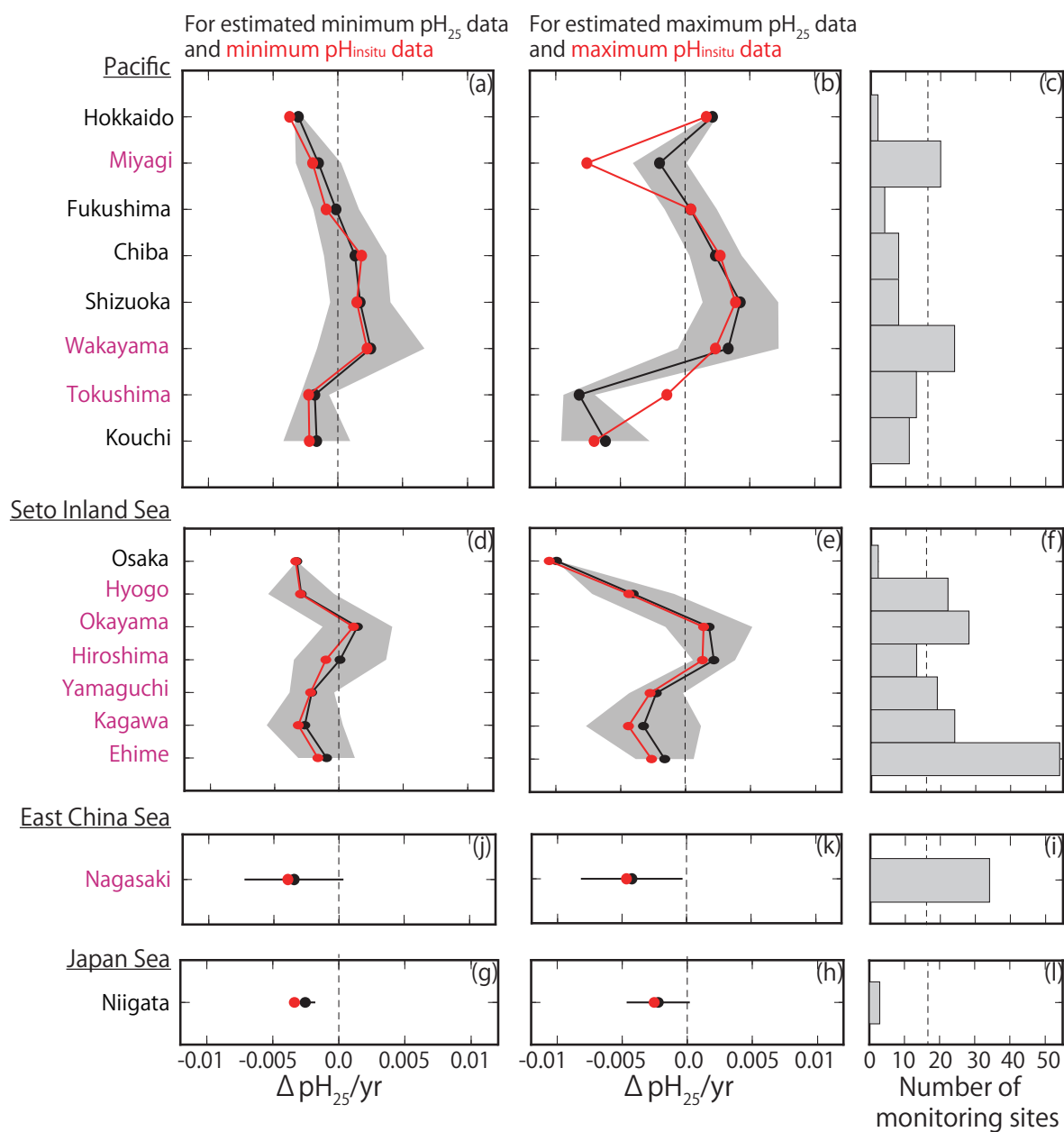


Fig. 11 (a–b, d–e, g–h, j–k) Same as Fig. 9, but showing the average estimated minimum and maximum pH_{25} trends ($\Delta \text{pH}_{25}/\text{yr}$) for each prefecture. Red lines and points indicate the average minimum and maximum $\text{pH}_{\text{insitu}}$ trends shown in Fig. 9.

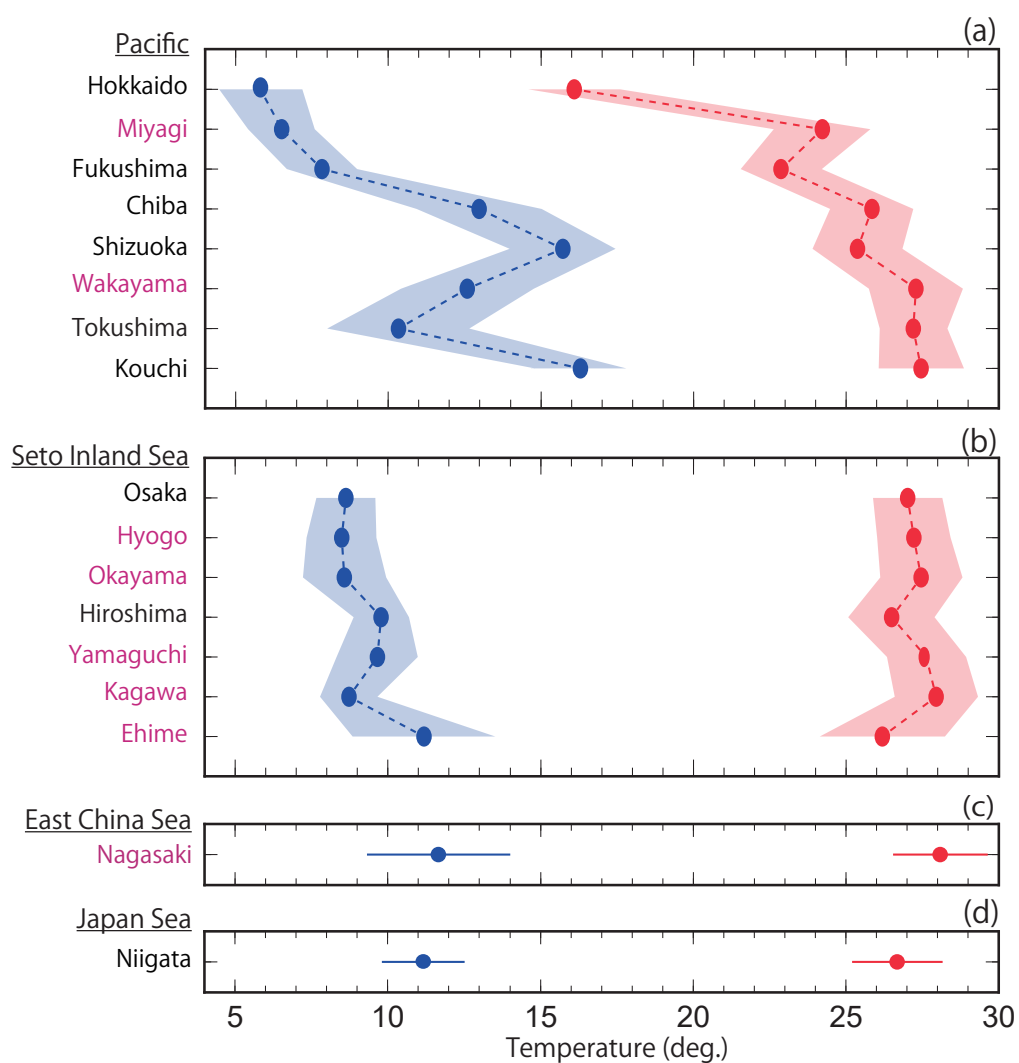


Fig. 12 Average highest and lowest temperatures observed for the minimum and maximum $pH_{in\ situ}$ data for each prefecture. The blue and red lines and shading indicate the average and one standard deviation from the average, respectively. The prefectures that met the threshold of 17 are shown in purple, as in Figs. 9 (c-l) and 11 (c-l).

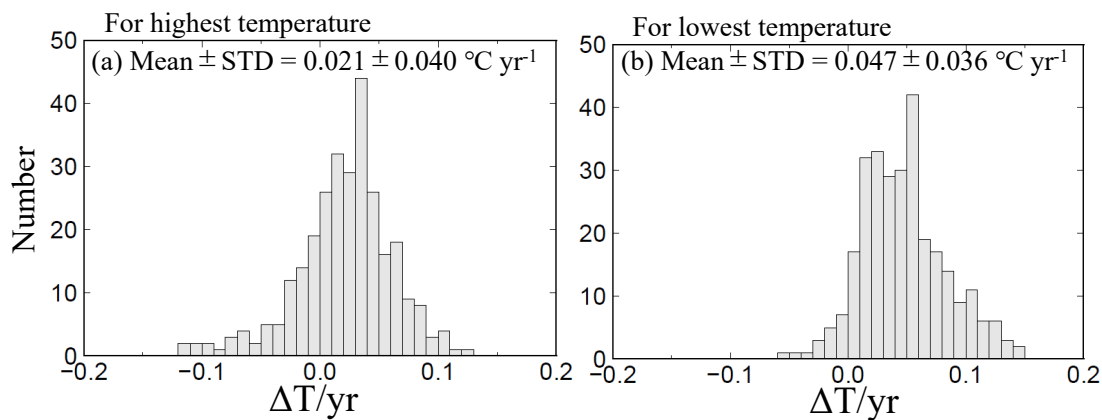


Fig. 13 Same as Fig. 7, but showing the highest and lowest temperature trends at 289 sites (selected by quality control step 3).

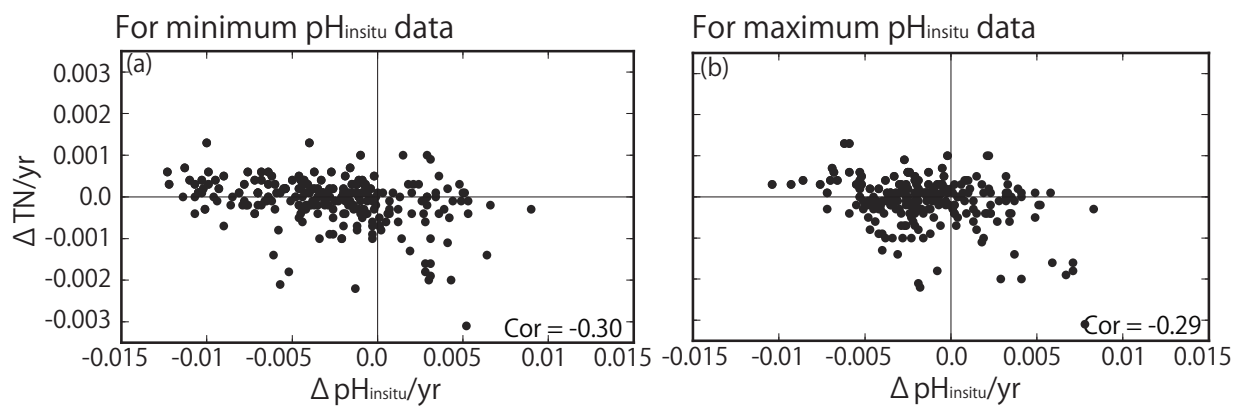


Fig. 14 Correlation between trends in total nitrogen (TN) and trends in (a) minimum and (b) maximum pH_{insitu}. The correlation coefficients are -0.30 and -0.29 for the minimum and maximum pH_{insitu}, respectively (significance level of 0.05, $r = 0.128$; degrees of freedom = 236).



Table 1 Number of samples (N) collected at each of the 1481 monitoring sites each year.

Year	$0 \leq N < 4$	$4 \leq N < 8$	$8 \leq N < 12$	$12 \leq N < 16$	$16 \leq N < 20$	$20 \leq N < 24$	$24 \leq N < 28$	$28 \leq N < 32$	$32 \leq N < 40$
1978	43	391	83	303	87	15	176	9	4
1979	31	372	73	328	101	19	150	11	7
1980	32	363	88	324	101	15	192	12	5
1981	24	347	72	361	99	13	199	11	3
1982	25	350	74	364	93	9	206	11	4
1983	32	355	75	356	91	11	222	12	0
1984	28	362	74	355	96	10	211	11	3
1985	24	354	86	377	96	9	192	11	8
1986	25	361	81	334	98	8	235	11	9
1987	26	357	78	341	98	4	239	11	1
1988	25	366	74	356	82	6	236	11	2
1989	26	365	83	344	84	5	238	17	3
1990	24	377	76	347	83	1	238	14	5
1991	24	367	80	355	93	5	226	13	5
1992	24	367	79	352	95	1	230	16	0
1993	17	374	76	357	94	8	225	14	0
1994	17	376	85	347	102	24	208	14	3
1995	29	376	109	311	104	3	227	12	0
1996	19	419	80	307	104	4	226	14	1
1997	20	396	82	315	115	5	225	13	0
1998	16	389	103	325	99	0	225	12	0
1999	17	396	68	381	67	2	224	12	7
2000	17	389	82	376	72	1	231	6	2
2001	17	392	90	382	50	8	220	6	1
2002	17	368	102	392	49	1	229	7	0
2003	17	365	93	402	51	1	233	6	1
2004	17	370	84	400	50	1	240	5	2
2005	16	354	152	356	46	9	228	3	0
2006	16	370	134	345	50	0	244	5	3
2007	17	399	128	353	62	0	202	5	3
2008	17	402	128	350	64	0	211	5	1
2009	17	403	143	340	58	0	217	5	8



Table 2 Average mutual correlation coefficients among water temperature and $\text{pH}_{\text{insitu}}$ at adjacent monitoring sites in the same prefecture. The averages were calculated from the data for the highest and lowest temperature, and minimum and maximum $\text{pH}_{\text{insitu}}$ within 15 km for the three criteria. We refined the sites using three quality control steps, yielding 1481 (step 1), 1127 (step 2), and 302 (step 3) sites.

Quality check procedue	highest temperature data	lowest temperature data	minimum $\text{pH}_{\text{insitu}}$ data	maximum $\text{pH}_{\text{insitu}}$ data
1	0.79	0.78	0.51	0.64
2	0.8	0.79	0.54	0.69
3	0.85	0.87	0.62	0.72



Table 3 Average correlation coefficients between minimum and maximum $\text{pH}_{\text{insitu}}$ trends and total inorganic nitrogen (TN) ones, respectively. We evaluated this for the data after each quality check procedues. Degree of freedom in step 1 and 2 are same values, because TN data are not necessarily measured at the whole of $\text{pH}_{\text{insitu}}$ monitoring sites. The sampling number of monitoring sites at step 1 and 2 were therefore the same number. Significant level, $\alpha = 0.05$ and degree of freedom are also represented.

Quality check procedue	Correlation between minimum $\Delta \text{pH}_{\text{insitu}}$ and ΔTN	Correlation between maximum $\Delta \text{pH}_{\text{insitu}}$ and ΔTN	Significant level of 0.05	Degree of freedom
1	-0.015	-0.29	0.08	622
2	-0.015	-0.29	0.08	622
3	-0.33	-0.35	0.14	215